DTIC FILE COPY

(2)

'ATION PAGE

Form Approved
OMB No. 0704-0188

AD-A231 883

DATE	3. REPORT TYPE AND DATES COVERED
31 Dec 90	Final Tech 01Sep86 to 31Mar90

4. TITLE AND SUBTITLE

Bonding at Metal-Ceramic Interfaces
in Hybrid Materials

5. FUNDING NUMBERS

(G) AFOSR-86-0321

6. AUTHOR(S)

Rishi Raj

7. PERFORMING ORGANIZATION NAME(S) AND ADDRESS(ES)

Cornell University
Department of Materials Science and Engineering
Ithaca NY 15853-1501

8. PERFORMING ORGANIZATION REPORT NUMBER

AFFINAL90

AFOSR-TR- 91 0036

9. SPONSORING/MONITORING AGENCY NAME(S) AND ADDRESS(ES)

AFOSR/NE
Building 410
Bolling AFB DC 20332-6448
Attn: Dr. A. H. Rosenstein

10. SPONSORING/MONITORING AGENCY REPORT NUMBER

2306/A1

11. SUPPLEMENTARY NOTES

12a. DISTRIBUTION/AVAILABILITY STATEMENT

Approved for public release;
distribution unlimited.

12b. DISTRIBUTION CODE

13. ABSTRACT *(Maximum 200 words)*

Abstract

Mechanical properties of metal-ceramic interfaces were measured at high temperatures. New methods were developed to measure the time and strain rate dependent properties of metal-ceramic interfaces under shear loading and under tensile loading. The shear experiment consisted of depositing a film of the ceramic on the metal and stretching the metal until periodic cracks developed in the ceramic film. Experiments on the copper/silica system demonstrated that these interfaces slide at high temperatures, with a linear relationship between sliding rate and the interfacial shear stress. In tensile experiments, bicrystals of copper and sapphire were loaded in tension. A threshold stress for fracture was measured. The room temperature properties of the interface were drastically altered by the precipitation of a very thin layer of an intermetallic. The formation of the intermetallic depended not only on the temperature but also on the oxygen partial pressure.

14. SUBJECT TERMS

Interfaces, MMC, Intermetallics, Oxidation,
Grain Boundary Sliding, Composites, Fracture

15. NUMBER OF PAGES

8+App. A,B,&C

16. PRICE CODE

17. SECURITY CLASSIFICATION OF REPORT	18. SECURITY CLASSIFICATION OF THIS PAGE	19. SECURITY CLASSIFICATION OF ABSTRACT	20. LIMITATION OF ABSTRACT
Unclassified	Unclassified	Unclassified	SAR

91 2 12 047

FINAL TECHNICAL REPORT

(9/1/86-3/31/90)

BONDING AT METAL-CERAMIC INTERFACES IN HYBRID MATERIALS

AFOSR-86-0321

Prepared for: Air Force Office of Scientific Research
410 Bolling Air Force Base
Solid State Division
Washington DC 20332

Attn: Dr. A. H. Rosenstein

Prepared by: Professor R. Raj
Department of Materials Science and Engineering
Cornell University
Ithaca NY 14853-1501

SUMMARY

Introduction

One of the important findings of a workshop on metal-ceramic composites, held at Aurora NY in September 1990, was that much greater emphasis must be placed on understanding the mechanical properties of MMCs at high temperatures. Th\ study of interfaces is particularly important at high temperatures because they are prone to shear sliding and creep embrittlement. The lead talk at this workshop described how the development of superalloys evolved into single crystal castings in order to eliminate the fracture and creep phenomena associated with grain boundaries.

This Air Force basic research program at Cornell University is dedicated to the study of high temperature mechanical properties of metal-ceramic interfaces. We are especially interested in time dependent phenomena such as shear sliding and void nucleation and growth that are related to diffusional mass transport at such interfaces.

In June 1990 this principal investigator visited WPAFB and submitted a report on the areas where research in MMCs needs to focus. Interface Science and Engineering, the subject of this research program, was one of the four areas (the others being constrained deformation, fiber science, and oxidation resistance) that were recommended for study. A copy of this report is attached as Appendix A.

The principal accomplishments of this research effort have been in the characterizing the phenomenology of time dependent mechanical properties of metal-ceramic interfaces. Two types of experiments, one for characterizing shear properties and the other for characterizing tensile

behavior have been designed and implemented. While some questions still remain about the details of these techniques, they are simpler than other methods available in the literature and the information obtained from them can be directly used to model and predict the mechanical response of continuous fiber metal-ceramic composites. Current experimental work has been limited to model material systems: copper/silica, copper/sapphire, and platinum/nickel-oxide.

We have also made good progress in relating mechanical properties to the atomistic structure of the interface. In the platinum/nickel-oxide system we have found that introducing a very thin layer of the intermetallic NiPt by suitable heat-treatment, increases the room temperature strength of the interface by a factor of four to ten. These results clearly show that intermetallics bond more strongly to oxides than simple metals.

Highlights

The three main results are summarized below. The first two have not yet been submitted for publication; therefore, the preliminary reports on them are included as Appendix B and C. The third result was recently published in Acta Metallurgica. A patent that was filed in December 1990 is briefly described under a separate section.

(a) **Strain Rate Dependent Sliding of a Metal-Ceramic Interface at High Temperatures.** A new technique developed at Cornell for measuring the shear properties of metal-ceramic interfaces was applied at high temperatures. The technique is described in Ref. 1 (see below); it consists of depositing a thin film of the ceramic on the metal and deforming the metal in tension. The ceramic film develops periodic cracks aligned normal to the pulling axis and the spacing of the

cracks is related to the shear stress supported at the interface. The following equation describes this relationship:

$$\tau_{mc} \quad \pi\sigma_f \frac{\delta}{\lambda} \tag{1}$$

where τ_{mc} is the shear stress supported at the interface, δ is the thickness of the ceramic film, λ is the spacing of the cracks in the film, and σ_f is the fracture stress of the film (also measured in the experiment). In the time dependent experiment the spacing, λ, and therefore the shear stress becomes strain rate dependent. From this information the sliding viscosity of the interface can be measured. The technique was applied to the copper/silica system. We found that sliding behavior at the copper-silica interface fell into two regimes. At slow strain rates and high temperatures, the stress supported at the interface increased linearly with the applied strain rate. At high strain rates, the interface stress became independent of the strain rate. The slow strain rate behavior was successfully explained in terms of a diffusional model where sliding is accommodated by transport of copper atoms around the non-planar asperities in the interface geometry.

(b) **Fracture at Copper-Sapphire Interfaces at Elevated Temperature.** The time dependent mechanical properties of the copper-sapphire interface in tension were obtained by diffusion bonding single crystals of copper to sapphire, and by applying dead weight loading normal to the plane of this "bicrystal". These experiments show a threshold stress for fracture. Below the threshold stress, which is of the order 10 MPa, the fracture time is very long, while above it fracture occurs only in a few minutes. If this result is general, it

would have major implications in the design and application of MMCs at high temperatures. The fast fracture above the threshold has been explained in terms of local diffusion at the crack tip. The apparent durability of the interface below the threshold is perplexing since cavities are seen to form but they do not grow with time. We are investigating the possibility of the growth of an intermetallic or a spinel layer at the copper/sapphire interface that alters the transport properties of the interface.

(c) **Control of the Mechanical Properties of Metal-Ceramic Interfaces Through Interfacial Reactions**. In collaborative work with Prof. Sass we have demonstrated that the shear strength of a metal ceramic interface can be changed by changing its structure at the atomic level. Specifically a reaction between platinum and nickel-oxide was used to form a very thin layer of the intermetallic NiPt at the interface. Even a one nanometer thick layer of NiPt increased the shear strength of the interface by a factor of 5 to 10 at room temperature. This result raises new theoretical questions about the relationship between the physical strength and the bonding between the atoms at metal-ceramic interfaces.

Publications

D. C. Agrawal and R. Raj
Measurement of the Ultimate Shear Strength of a Metal Ceramic Interface
Acta Metallurgica et Materiala, 37, [4], 1265-1270 (1989)

D. C. Agrawal and R. Raj
Autonucleation of Cavities in Thin Ceramic Films
Acta Metallurgica et Materiala, 37, [7], 2035-2038 (1989).

C. M. Kennefick and R. Raj
Copper on Sapphire: Stability of Thin Films at $0.7T_m$
Acta Metallurgica et Materialia, vol 37, [11]. 2947-2952 (1989)

F. S. Shieu, R. Raj and S. L. Sass
Control of the Mechanical Properties of Metal-Ceramic Interfaces through Interfacial Reactions
Acta Metallurgica et Materiala, 38, [11], 2215-2224 (1990).

Patent

The following is an abstract of a paper entitled "Transition Metal Thin Films on Oxides" that is being prepared for a publication. It is based upon a patent entitled "Metal Coated Ceramic Substrates" that was filed at the U. S. Patent Office in December 1990.

"In this brief paper we describe how we were able to prevent the beading of thin palladium films on sapphire by co-depositing aluminum with the palladium. The aluminum metal is believed to have accelerated the formation of an intermetallic by reducing the local oxygen activity. Surprisingly the co-deposited films remained continuous even when annealed in air, since that should have led to the oxidation of the intermetallic into aluminum-oxide and platinum. It is proposed that the intermetallic forms a low energy interface with the sapphire which preempts beading. The approach presented here may be useful in many technologies ranging from catalysis to the processing of metal ceramic composites by liquid metal infiltration."

(The rights to this information and patent lie with the Cornell Research Foundation).

Graduate Students

Christine M. Kennefick has been supported full time from the AFOSR Grant. Partial support was also provided to L. Parks and V. Jobin.

Professor D. C. Agrawal received summer support as a visiting scholar from this grant, and research technician Glenn Swan was partially supported from the AFOSR Grant.

Plans

We plan to work in three areas: (i) Continuation of the measurement of the time and strain rate dependent mechanical properties of metal-ceramic interfaces and their relationship to the atomic structure of the interface. (ii) Developing a detailed understanding of how reactions at the interface that form thin layers of intermetallics are controlled by temperature and the oxygen partial pressure, and how the presence of this intermetallic influences the high temperature mechanical properties of the interface. (iii) Modeling and conducting experiments with model composites made from continuous ceramic fibers. Predicting the properties of such composites from information obtained from the periodic cracking experiments described in this report.

Appendix A

A Report on Metal Matrix Composites

to

Dr. D. Dimiduk

WRDC/MLLM

WPAFB, OH 45433

July 1990

Raj (Cornell) to Dimiduk (WRDC/MLLM)

WPAFB Visit/June 18-22, 1990

SUMMARY

This report summmarizes findings and recommendations for metal-matrix composite research based on a recent, week long visit to the Air Force Materials Laboratory. In addition to suggesting specific research directions, the report recommends that the materials laboratory should provide national leadership in crossdisciplinary research and graduate education in the field of high temperature structural materials.

Four specific areas are recommended. These are interface science and engineering, constrained deformation, fiber science and oxidation resistance. All in some form are current research concerns of the Air Force Laboratory. The goal of materials design requires that they be studied with an interdisciplinary focus, rather than as isolated areas geared solely toward understanding materials behavior.

The goal of interface science and engineering is to understand and control properties of the interface. Theoretical calculations of interfacial adhesion at the atomic level, observation of interfacial reactions, and the time and temperature dependent mechanical properties of interfaces should be studied.

Constrained deformation research in composite materials is important because the rigidity of the ceramic fibers can constrain deformation in the metal. Both the extent of the deformation and the state of stress at which it occurs determines the composite toughness. Research should include both theoretical and experimental work on model systems. It is important to note that the techniques used to synthesize model materials may differ from those used to fabricate engineering materials.

Progress in new composites is likely to be limited by the high temperature mechanical properties of the fiber. Breakthroughs will come only when we understand fiber science, specifically the degree to which a fiber may contain defects but yet perform well in a composite. In certain cases, a highly oriented grain structure may work as well as a single crystal fiber. Criteria for fiber microstructure design must be established.

Oxidation resistance of high temperature structural materials depends on how oxygen diffuses along the interface and how the concentration of oxygen affects mechanical properties.

Thermodynamics and kinetics of interfacial reactions must be studied as a function of oxygen partial pressure and their influence on mechanical properties of the interface needs to be characterized.

These four areas are best studied with an interdisciplinary focus, a goal which can be realistically pursued at the Materials Laboatory in view of the ongoing breadth of activities in synthesis micromechanics and mechanics of advanced structrual materials. A natural ougrowth of this focus can be to train young scientists. Our nationwide Ph.D. shortage in high temperature structural materials is an acute concern, and requires an educational mission for a laboratory of this stature. The crossdisciplinary nature, the impressive breadth, and the intensity of in-house research activities at WRDC can make it the national center for both research and education in the field of the temperature structural materials.

Introduction:

The objective of the visit was (a) to meet and discuss research in the area of high temperature structural materials with scientists at WPAFB/WRDC/MLLM and (b) to highlight ongoing efforts and to suggest new opportunities for interdisciplinary fundamental research that can be successfully pursued at the laboratory.

The scientists I met and the topics discussed were as follows: J. Larsen (mechanical properties of metal-matrix composites), V. A. Krishnamurthy (mechanical properties of metal-ceramic interfaces), Y. W. Kim (processing of metal-ceramic composites), M. Mendiratta (niobium silicide based materials), P. Smith (titanium aluminide ceramic composites), C. Woodward (electronic structure calculations), T. Nicholas (continuous fiber metal ceramic composites), D. Miracle (crystal slip boundary

interactions), and R. Kerans (interface mechanics). Throughout the week, several discussions were held with Dennis Dimiduk, who kindly served as an enjoyable and purposeful host.

The discussions were informal. Specific, as well as broad issues, were discussed. Before delving into specific research topics, I will give a personal view of the role of fundamental research in the development of new, high performance structural materials. At the end of this report, I will emphasize the need for Ph.D. graduates in this field.

The Importance of Fundamental Research in the Development of New, High Performance Structural Materials:

Directionally solidified nickel base superalloys for blade applications represent the state-of-the-art high temperature structural material. Its microstructure consists of unidirectional grains containing large volume fractions of an intermetallic phase. The deliberate orientation of the interfaces reduces the shear and tensile traction to a minimum during service; thereby ameliorating the effect of the poor mechanical properties of the interfaces.

The search for new materials is likely to progress on two fronts. The first will parallel the development of superalloys, where nickel based materials will be replaced by refractory metals and

their intermetallics. This work is in its infancy.

Fundamental research of the following topics will be important in the development of these new materials: (i) mechanical properties of the intermetallics and (ii) mechanical properties of the refractory metals doped with small concentrations of the other element either in solid solution or in the form of fine precipitates of the intermetallic.

The advent of ceramic fibers has opened up a new frontier for the design, research, and development of innovative, high temperature structural materials. Controlled properties in these materials will most likely require the use of continuous fibers. The fascination of these materials is that the properties of the composite depend upon the interaction between the properties of the constituents and not just on their absolute properties. For example, putting the strongest fiber in the strongest matrix along with a strong interface will not necessarily give the optimum composite. The fundamental research on these materials should, therefore, begin with materials design. The purpose of the research should be to develop basic rules and criteria for optimizing the properties of the composite. Experimental research should also focus on the development of these concepts with highly controlled microstructures, preferably on model systems. Clearly, the success of the fundamental work would depend upon the ability to synthesize highly controlled

microstructures.

As we enter the age of new materials, fundamental research must not only provide an understanding of the atomistic mechanisms of deformation, it must also provide the basic criteria for the optimal design of new materials that are made from metals, intermetallics and ceramics. These basic conceptual designs can, and will, steer innovative research toward the development of new engineering materials.

In the following sections, topics that can form the components in materials design are discussed. Each topic is in some way, already being pursued at WRDC-MLLM. The topics are interface science and engineering, constrained deformation, fiber science, and oxidation resistance.

Interface Science and Engineering:

The importance of the interface in controlling the composite's mechanical toughness is illustrated in Figure 1. In it, the properties of the matrix, the fiber and the composite are shown schematically. The tensile ductility and the yield strength of the composite lie in the region that is intermediate between the properties of the fiber and the matrix, often closer to the properties of the fiber than the matrix. However, the "toughness" of the composite, can be much greater than it is for

either the matrix or the fiber. The enhancement in the toughness depends on shear and tensile properties of the interface. A change in the properties of the interface due to oxidation, for example, can have a dramatic effect on the toughness of the composite.

In general, the interface must be characterized in terms of (a) the atomic structure and the local chemistry of heterointerfaces and (b) the width of the interface layer compound if such a compound is present. This compound can be a deliberate coating on the fiber or it may be produced by in-situ reaction under controlled oxygen activity and temperature. Its width can vary from a few atom monolayers to several thousand atom layers. The interface layer plays an indirect role in controlling adhesion at the interface. The atomic structure and chemistry of the interface next to the ceramic fiber can be designed by controlling the composition of the interface layer. The interface layer can also preserve the properties of the interface by serving as a buffer, thus inhibiting reactions between the fiber and the matrix and inhibiting oxygen diffusion at high temperatures.

Thus interface research must include theoretical calculations of the effect of interface chemistry on adhesion, the study of the reactions at the interface, and the measurement of the time dependent shear and tensile properties of the interface.

The theory of the cohesive strength of metal ceramic interfaces should emphasize electron density calculations by an ab-initio approach, exemplified by the LMTO approximation. Such calculations have been carried out at Max Planck Institute and have yielded interesting results for silver-magnesium oxide and nickel-nickelsilicide interfaces. The electron structure approach is more useful than the pair-potential approach for these interfaces because the bonding depends only partially on the atomic arrangement of atoms at the interface. The strength of the different types of bonds and the role of impurity atoms (for example, titanium) on the strength of the local bonds is an important factor in determining interfacial adhesion.

At high temperatures chemical reactions at the interface can change its properties. The thermodynamic driving forces and the rate of these reactions depend upon oxygen activity because the reaction involves a metal (A) and a metal-oxide (BO). The role of oxygen (O) activity is particularly important when A and B can form an intermetallic. The rate of these reactions can be studied, for example, by depositing thin films of one material on the other and following the reaction kinetics by Rutherford Backscattering Spectroscopy. These techniques have been routinely used to study reactions in multilayer electronic devices. They can be used just as well for structural materials.

At least three methods for measuring the mechanical properties of

interfaces have been reported in recent literature. They are the indentation method, the periodic cracking method, and the laser ablation method. The indentation method was developed first and is the best understood. It is applicable to fibers embedded in stiff matrices. Although the technique may work for ceramic fibers in a titanium aluminide matrix, it may not be successful if the matrix has a low yield stress. The periodic cracking can be applied to films or to fibers. This method is most suitable when the matrix has a plastic ductility of a few percent. The technique has been used to measure properties at elevated temperatures and is yielding information on the viscosity of sliding at metal-ceramic interfaces. The laser ablation technique is the most recent and relies on the decohesion of the metal film from a ceramic surface as a result of thermal stress that develops when the film is heated by a laser beam. The technique is complex since it requires a knowledge of the optical absorption properties of the ceramic and the metal. As a result of these and other techniques that may be developed, our ability to characterize the mechanical properties of interfaces continues to improve.

In summary, the subject of interface science and engineering should be pursued on its own. Theoretical calculations of interfacial adhesion, an understanding of interfacial reactions and the measurement of the time dependent mechanical properties of the interfaces are topics that warrant further study.

Constrained Deformation:

The enhancement in the toughness of the composite, illustrated in Fig. 1(c) is a result of the dynamic interaction between deformation in the metal phase and the concomitant decohesion at the metal ceramic interface. The majority of the work of fracture in the composite in a tensile test is expended in the deformation of the metal. Thus, the larger the volume of the metal involved in deformation, the higher the strain and the greater the applied stress, the greater is the work of fracture. All of these factors depend not only upon the intrinsic properties of the metal matrix, but also upon the local constraint exerted by the ceramic interfaces on metal deformation. This constraint increases the hydrostatic component of the local stress which, in turn, requires a larger applied stress to achieve plastic flow. However, if the constraint is too large, then the volume of the metal participating in the plastic deformation becomes very small. Thus optimum design requires a balance between the strength of the interface and the yield strength of the metal. This point is illustrated schematically in Fig. 2, which illustrates the possible load displacement curves for various interactions between yield stress and the interfacial strength. The graph assumes that the intrinsic ductility of the metal scales inversely with its yield strength - in reality, both can be varied independently to a limited extent. It shows that at a given yield strength of the

metal, the yield strength of the composite increases with interfacial cohesion; this is because a higher interface strength enhances the constraint on the deformation of the metal. However, the work of fracture, which equation is the product of the applied load and the resulting displacement, is maximized when the local yielding in the metal and the decohesion occur together; this is most likely when the interfacial strength and the yield stress of the metal are nearly equal.

The problem discussed above can be addressed quantitatively by finite element simulations of elastic-plastic deformation. Results from these calculations must then be combined with experiments on model systems in order to develop the criteria for the design of new composite materials.

The objective of experiments with model microstructures requires facilities for making materials in which the geometrical features of the microstructure as well as the composition can be controlled at the atomic level. Since the objective of the fundamental work ought to be to test conceptual material designs, the techniques used to synthesize and test model materials should not be constrained by traditional methods.

Fiber Science:

The evolution of new structural materials is likely to fall into

two categories, one of them having the two phase microstructure that resembles the superalloys, and the other being fabricated from continuous fibers. In the second case the availability of new fiber materials will limit the development of high performance structural materials. Ideally, the fibers should be free from grain boundaries since boundaries slide and fracture at high temperature. At the present time, much of the research is centered around polycrystalline silicon carbide fibers and single crystal sapphire fibers.

Research on fiber science should address the question of the synthesis and the use of fibers that consist of a highly elongated grain structure. Such fibers should have the same high temperature mechanical properties as single crystal fibers in uniaxial tension. In off axis loading, the texture in the fibers should make them better than the single crystal fibers. The advantage of the oriented fibers is that metallurgical processing techniques may be used to make them; the general idea being to induce preferred grain growth along the fiber direction through thermomechanical processing. In addition, new methods such as grain seeding and direction crystallization can be conceived for making oriented single crystal fibers. This area offers many opportunities for fundamental research centered on controlled grain growth in the solid state and spans across all materials including ceramics and intermetallics.

Oxidation Resistance:

The oxidation resistance of high temperature structural materials is related not only to the growth of an oxide scale, but also to the diffusion of oxygen at interfaces and its effect on the mechanical properties of the interface. In nickel base superalloys oxygen is believed to react with carbide precipitates in grain boundaries to produce carbon monoxide of high fugacity, which promotes the nucleation of cavities. Although we do not understand why boron improves the oxidation resistance of superalloys, one explanation is that it lowers both the concentration and diffusivity of oxygen at interfaces.

In the case of composites made from silicon carbide fibers, the presence of a carbon layer at the metal ceramic interface has obvious connections to interface oxidation.

The fundamental research on oxidation resistance should focus on the effect of the chemistry of interfacial reactions under controlled oxygen activities. Similarly, environmental effects in high temperature mechanical behavior must be characterized in terms of the oxygen activity in the environment so that the mechanical behavior can be related to interfacial reactions. Oxygen activity in the environment can be controlled by gas mixtures (carbon monoxide and carbon dioxide mixtures or hydrogen with a controlled dew point) or by solid state buffers. It can

range from 10^{-18} or lower, up to one atmosphere. The transitions in mechanical behavior with oxygen activity can provide the impetus for understanding chemical reactions at the interface.

In Conclusion:

The technological prowess of America will continue to depend upon its ability to attract and train the best minds in the cutting edge of technologies. Space exploration must be viewed as an arena where America, Europe, and Japan will compete. Aerospace transport technologies will form the first link in this human endeavor. The availability of innovative, high performance structural materials will be one of the key factors in the development of new vehicle technologies.

I am concerned that we are not training doctoral students in the area of high temperature structural materials. In the past, the superalloys provided an incentive for government agencies to support fundamental research at universities. But the future mission for fundamental research in structural materials is more diffuse. The new focus should be guided more by our potential to create new materials rather than being limited to understanding the failure mechanisms of existing materials.

The Materials Laboratory at Wright Patterson is in a unique position to become the national champion for doctoral education

in structural materials. The local experience is extensive and unique in many areas that range from different materials to different aspects of the study of structrual materials. The contact with the NASP program gives the WPAFB scientists a feel for the engineering problems and creates and excitement for innovative materials. I believe that the Materials Laboratory has a national role in promoting interdisciplinary research and education in structural materials made from metals, intermetallics, and ceramics.

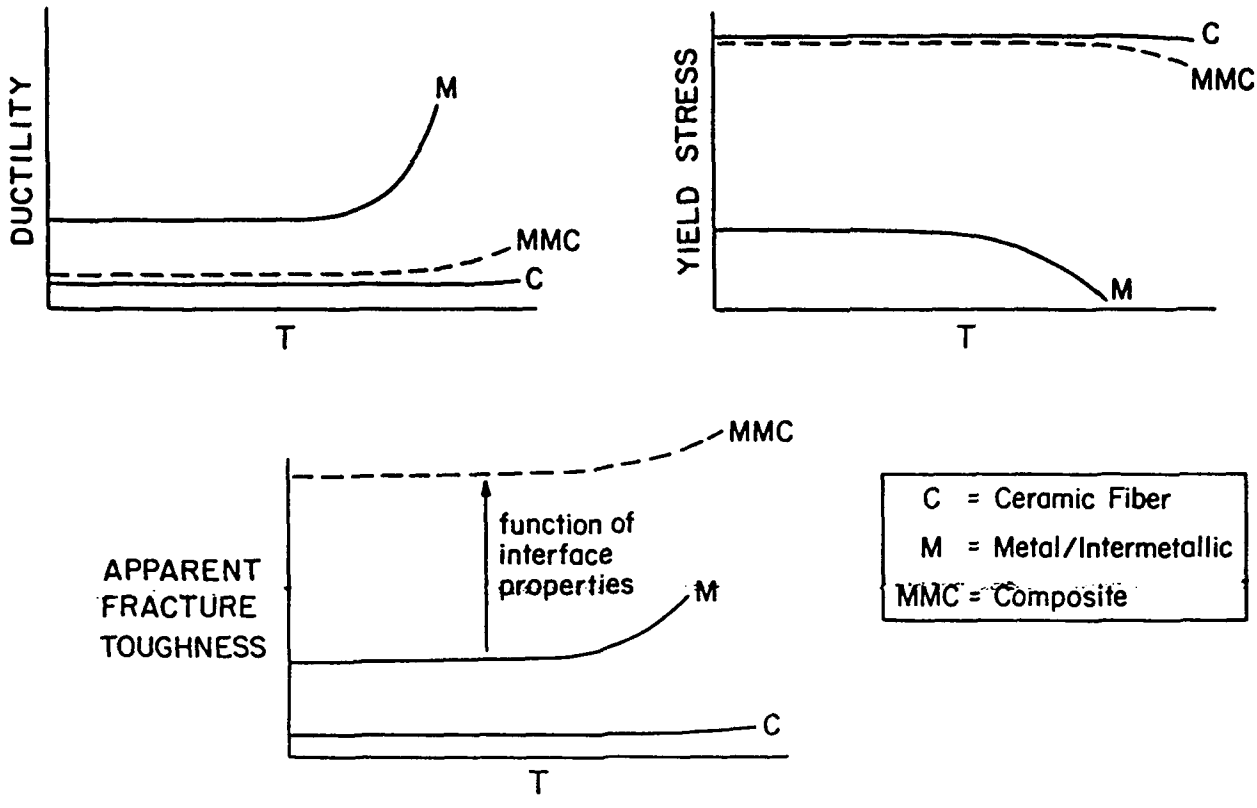

Figure 1: Schematics illustrating the ductility, the yield stress, and the apparent fracture toughness of the metal/intermetallic, the ceramic fiber and the continuous fiber composites, as a function of temperature. The ductility and the yield stress of the composite lie close to the properties of the ceramic, but the toughness can be much greater than either the metal or the ceramic. The enhancement in toughness depends upon the properties of the interface.

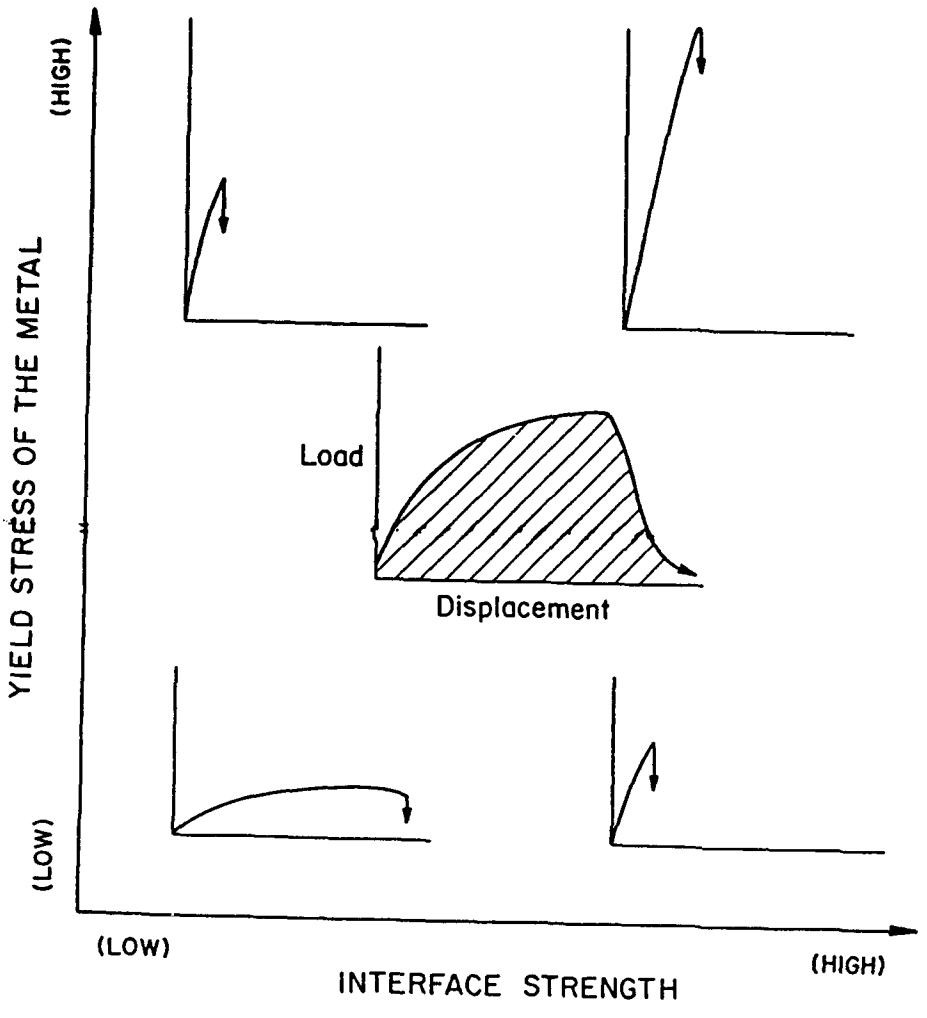

Figure 2: Schematics showing the effect of the relative yield stress of the metal and cohesive strength of the interface on the load/displacement curves for fiber reinforced composites. A high interface strength increases the constraint on the deformation of the metal, thereby increasing the yield strength of the composite. However, the highest work of fracture is obtained when decohesion and deformation in the metal occur concomitantly, as illustrated by the schematic in the center.

Appendix B

Fracture of Copper-Sapphire Interfaces at Elevated Temperatures

C. M. Kennefick and R. Raj

to be submitted for publication in Spring 1991

FRACTURE AT COPPER-SAPPHIRE INTERFACES AT ELEVATED TEMPERATURES

C. M. Kennefick and R. Raj
Department of Materials Science and Engineering
Cornell University
Ithaca, NY 14853

Abstract

The fracture characteristics were examined for single crystal and polycrystalline copper-sapphire specimens hung in tension from 500 to 800°C. When either the stress or temperature was varied, the fracture mode exhibited an abrupt transition from a pore growth process to brittle fracture. The threshold stress for brittle fracture was found to be 1.6 MPa lower for polycrystalline copper than for single crystal copper and 1.3 MPa higher at 700°C in a hydrogen and argon gas mixture than in high purity argon. Below the threshold stress, inhomogeneities in the size and distribution of pores, along with the calculated stress to nucleate a thermodynamically stable pore being higher than the applied stress, indicated that pore growth was influenced by stress concentrations. The low threshold stresses for rapid failure were found to be in agreement with the thermodynamics of brittle fracture. A model involving surface and interfacial diffusion to help explain the decreasing threshold stress with increasing temperature is developed.

Introduction

At about half their melting points polycrystalline metals will exhibit a minimum in ductility caused by the diffusive growth of voids and cracks. It has been shown for metallic materials with a fixed array of pores with spacing λ that the time to fracture should be proportional to λ cubed and should be inversely proportional to the applied stress [1]. Since the growth of the pores involves the diffusion of metal atoms along the grain boundaries, the time to fracture was also shown to be proportional to the grain boundary diffusion coefficient D_b. Thus fracture time as a function of applied stress, as shown experimentally by Raj [2] on copper bicrystals, will yield information on the diffusion of metal atoms governing the growth of pores.

The purpose of this study was to characterize pore nucleation and growth at a metal-ceramic interface at high temperatures. It was found, however, that the mode of fracture was highly dependent on experimental conditions. When either temperature or stress was varied, the fracture would change abruptly from a process involving pore growth to brittle fracture that occurred within a few seconds. Interfacial diffusion of the metal atoms may therefore be involved in both pore growth at low stresses and crack advance or blunting at higher stresses.

It is shown that near the transition region pore growth in the metal may be coupled with the slow advance

of a crack along the interface. The surface of the metal was found by metallographic examination to have an inhomogeneous distribution in the sizes of pores, as exhibited by a region near one edge having pores coalesced with the density and size of pores decreasing away from this region until no pores were present. Furthermore, the minimum stress calculated to nucleate a stable pore of the size seen experimentally was greater than the applied stress. Both the inhomogeneous distribution of pores and the size of the smallest pores suggested that in the absence of grain triple junctions, grain boundary sliding, and slip bands near the pores, a stress concentration could be present from an advancing crack tip.

Cracks along the interface were found to propagate rapidly at lower threshold stresses as the temperature increased. A model is developed to show how interphase boundary diffusion and surface diffusion can operate simultaneously to promote brittle fracture at decreasing stresses with increasing temperature. The low threshold stresses themselves and a decrease in threshold stress for polycrystalline copper-sapphire specimens are modelled in terms of brittle fracture along the interface at high temperatures.

Experimental

The samples consisted of single crystal or polycrystalline discs of copper diffusion bonded to between two sapphire rods. Before bonding, both the ends

of the sapphire rod pieces and the faces of the copper disc were polished to 0.05 μm and cleaned by heating. The sapphire rods were heated in air to 1000°C and the copper discs were heated in an H_2 forming gas to 800°C.

For the sapphire pieces, a sapphire rod 1/8 inch in diameter and 6 inches long was first cut into two pieces, one 5 3/4 inches long and the other 1/4 inch long. The shorter piece was then diffusion bonded at 1700°C under a stress of 8.6 MPa to an alumina disc 1 centimeter in diameter. The disc on the end of the rod assembly would later sit on the end of an upright tube inside the furnace, thus allowing the sample to hang with weights attached to the other end during heating.

In making a specimen, a copper disc 3 mm in diameter and 1 mm thick was diffusion bonded between the ends of two sapphire rod pieces at 1000°C for 40 minutes under a stress of 8.6 MPa. These minimum conditions found for the copper-sapphire bond parallel those used earlier by Klomp [3]. Stresses 5 MPa or less at 1000°C or temperatures of 900°C or less at 8.6 MPa were found to bond the copper to the sapphire poorly or not at all.

The creep testing was done at temperatures from 500 to 800°C under stresses ranging from 1.8 to 4.6 MPa. In each test the sample was brought to temperature and then a constant weight hung from the sample end. The furnace, being only about 4 inches high, could be kept to within 1 degree of the testing temperature. The chamber containing the sample was sealed so that during heating, testing, and

cooling only high purity argon or a hydrogen and argon mixture flowed in the furnace from a gas inlet to an outlet.

Copper fracture surfaces were examined by scanning electron microscopy. Samples that did not break during testing were cleaved at the copper-sapphire interface before examination in the microscope.

Fracture Characteristics

When either the stress or temperature was varied, as shown in Figures 1 and 2, the fracture time at a particular point changed from over 24 hours to 1 to 3 seconds. Such a transition in fracture has also been observed in polycrystalline alumina [4], in which fracture at lower stresses was ascribed to pore growth and that at higher stresses to flaw controlled fracture. What is different in the metal-ceramic interface case is that beyond a certain stress the sample can fail almost instantly.

None of the specimens whose fracture times lie to the left of the curves in Figures 1 and 2 were tested until final fracture. In contrast to copper bicrystals which fractured in 2 to 120 hours [2], these copper-sapphire samples would hang without breaking sometimes more than three to five days or even two weeks. Each of the specimens tested for data points to the left of the transition regions, however, were left in the furnace for at least 24 hours.

The specimens that did not break and were subsequently cleaved for metallographic examination showed an inhomogeneous distribution in the size and density of pores, as shown in Figure 3. Also in contrast with the fracture of copper bicrystals and the fracture of metals above 0.4 T_m when the area fraction of cavities is 0.2 to 0.4 [5], the coalescence of pores at least in a small region of a copper-sapphire specimen did not lead to catastrophic failure. Although it is not certain after cleaving the specimen that a blunted crack may be present behind the pores, the presence of voids in a metal matrix composite [6] or ductile ligaments at a metal-ceramic interface [7,8] have been shown to increase the work to fracture, which may in part be contributing to the long fracture times just below the transition stress.

Except for specimens fracturing at 750 or 800°C, specimens fracturing in the transition region showed few if any pores. Some of these specimens did, however, show slip bands and striations (Figure 4), suggesting that the crack moved forward in separate stages.

The effect of adding a small amount of hydrogen to the argon atmosphere was to shift the threshold stress for brittle fracture 1.3 MPa higher at 700°C (Figure 5). Instead of embrittling the interface, the hydrogen may be producing a slightly reducing environment to offset any enhanced crack propagation caused by residual oxygen in the argon. The surface self diffusion of silver has been shown to be faster in an oxygen atmosphere than in a mixed

nitrogen and hydrogen atmosphere [9] so that if metal surface or interfacial diffusion is involved in crack propagation, the slower diffusion in an atmosphere with some hydrogen may help explain the higher threshold stress.

Pore Nucleation and Growth

The nucleation and growth of pores in the copper appear to be influenced by a stress concentration in the specimen. As mentioned earlier, very large pores can appear in localized areas. One such area, as shown in Figure 3, lies adjacent to the specimen edge.

The calculated stress required to nucleate a thermodynamically stable pore was found to be larger than the applied stress. The change in free energy needed to nucleate a pore with radius of curvature r at a polycrystalline metal-ceramic interface is

$$\Delta G = \gamma_m A_m - \gamma_{gb} A_{gb} - \gamma_{cm} A_{cm} + \gamma_c A_c - G_v V_p \qquad (1)$$

where γ_m is the metal surface energy, γ_{gb} the metal grain boundary energy, γ_{cm} the metal-ceramic interfacial energy, and γ_c the ceramic surface energy. A_m is the metal surface area created in nucleating the pore, A_{gb} the grain boundary area lost, A_{cm} the metal-ceramic interfacial area eliminated, and A_c the ceramic surface area exposed (Figure 6). V_p is the volume of the pore and G_v the free

energy per unit volume lost since the local traction σ_n does work in creating the pore. G_v can be written as

$$G_v = \sigma_n \tag{2}$$

The surface areas gained or lost in nucleating the pore can be written as

$$A = Fr^2 \tag{3}$$

where F is the relevant shape factor. Likewise the volume may be written as

$$V_p = F_v r^3 \tag{4}$$

Since $A_c = A_{cm}$ and

$$2\gamma_m \cos\alpha = \gamma_{gb} \tag{5}$$

where α is half the dihedral angle between the grains, a final expression for ΔG is

$$\Delta G = [\gamma_m F_m - 2\gamma_m \cos\alpha\, F_{gb} + (\gamma_c - \gamma_{cm})\, F_{cm}]\, r^2 - [\sigma_n F_v]\, r^3 \tag{6}$$

The critical radius r_{crit} at which the pore will not shrink is found by minimizing ΔG and is given by

$$r_{crit} = \frac{2[\gamma_m(F_m - 2F_{gb}\cos\alpha) + (\gamma_c - \gamma_{cm})F_{cm}]}{3\sigma_n F_v} \tag{7}$$

The contact angle ϕ between the metal and ceramic surface is often influenced by faceting and for copper beads on sapphire was seen to be 90 degrees [10], so that γ_c and

γ_{cm} were not related to γ_m in the above equation according to the Young-Dupre equation used for liquid metal droplets on ceramic surfaces. Although some of the pores may have been ellipsoidal, approximating their shapes as spherical caps in the single crystal metal case with $\phi = \pi/2$ and $\alpha = \pi/2$ leads to $F_m = 2\pi$, $F_{cm} = \pi$, and $F_v = 2/3\ \pi$. The critical radius may then be written as

$$r_{crit} = \frac{2\gamma_m + \gamma_c - \gamma_{cm}}{3\sigma_n} \qquad (8)$$

The critical radius from the above equation, using $\gamma_m = 1.913\ J/m^2$, $\gamma_c = 1.02\ J/m^2$ and $\gamma_{cm} = 1.93\ J/m^2$ [11] for copper on sapphire at 700°C, is 0.97 μm for $\sigma = 3$ MPa. The average value of r of some of the smallest pores from a specimen tested at 700°C was 0.41 μm, corresponding to a stress of 7.2 MPa. The average radius of the smallest pores from tests at 580 to 800°C ranged from 0.11 to 0.50 μm, corresponding to calculated stresses of 5.8 to 26 MPa.

These calculated stresses range from 2 to 8 times as high as the actual applied stress in each test. Since the threshold stress is greater than the applied stress, the nucleation of the pores should be occurring in the presence of a stress concentration [12], possibly from a crack tip since there are no grain boundary triple junctions or grain boundary sliding in the single crystal specimens.

Pore nucleation in the presence of stress concentrations may also be important in the case of

polycrystalline metals on ceramics. The probability of nucleating a single pore of critical size is given by

$$e^{-\Delta G_{crit}/N_p kT} \quad (9)$$

where N_p is the number of atoms removed in creating the pore. ΔG_{crit} may be found by substituting equation 7 into equation 6. For a contact angle ϕ of 90 degrees, the relevant shape factors for a three grain junction on a ceramic can be derived from those given by Clemm and Fisher [13].

Using the surface and interfacial energies for copper at 700°C used before and α equal to 75 degrees gives a ratio of the probability of nucleating a pore at a metal three grain junction on the ceramic to the probability of nucleating a pore in the single crystal of 1. Thus for α at 75 degrees shape factors approaching those of a hemisphere do not influence ΔG greatly and the rate of pore nucleation may therefore be influenced by stress concentrations in the specimen.

Such a prediction was verified by experiment as shown in Figures 7 to 9. The same transition from pore nucleation and growth to brittle fracture was seen for polycrystalline specimens, but the threshold stress for brittle fracture at 750°C was 1.6 MPa lower than that in the single crystal case. Thus below the transition point the pore nucleation and growth process was again very slow. In this case it was verified that at 750°C under a

stress of 1.02 MPa, just below the threshold stress, the time to fracture was greater than 2 weeks. For specimens fracturing in less than 30 seconds (Figure 9), open grain boundaries were seen over almost the entire fracture surface.

The ease by which a crack can run across the interface, facilitated by the opening of the grain boundaries, can be understood by considering the stress concentrations produced at triple grain junctions [14-16]. The shear stresses arising from initial loading are first relaxed by grain boundary sliding [14]. Since the sliding can be accommodated by elastic deformation only partially at triple grain junctions, elastic boundary tractions result which may be relaxed by diffusion. The sliding and stress concentrations set up at the metal-ceramic interface are analogous to those arising at the intersection of a grain boundary and a rigid second phase particle, only in this case the second phase may be considered planar with infinite extension at right angles to the boundary. The open grain boundaries seen experimentally may be the result of copper grain boundary sliding itself as the sliding intersects the sapphire phase or it may be caused by the subsequent rapid pore nucleation, growth, and coalescence at the boundary.

The normal traction at a triple grain junction to be relaxed by diffusional flow, $\sigma_n = \sigma_n(x,t)$, was derived by Evans et al. [15] and for $x = 0$ is

$$\sigma_n(0,t) = 1.38\ \beta\sigma_- \left(\frac{\tau_n}{t}\right)^{1/6} \tag{10}$$

In the above equation β is a constant and τ_n is a relaxation time given by

$$\tau_n = \frac{2\ell^3(1-\nu)kT)}{\mu\Omega D_b\delta_b} \tag{11}$$

where ℓ is the free length of sliding, ν Poisson's ratio, μ Young's modulus, Ω the atomic volume, and D_b and δ_b the grain boundary diffusion coefficient and width respectively. It is shown for nickel with grain size 50 μm, $\beta = 0.3$, and a temperature T of 0.70 T_m where T_m is the melting point, that the maximum boundary traction can be 10 to 100 times the applied stress. These same size stress concentrations, if occurring in the copper-sapphire case, could help explain the rapid opening of the grain boundaries promoting crack propagation.

That the boundaries open up within a few seconds is also in agreement with theory developed on relaxation of boundary tractions. For nickel with grain size 50 μm the characteristic relaxation time τ can be about 1 ms.[15] Raj shows in detail[16] that the blunting of initial tractions, owing to short diffusion distances and increasing grain boundary diffusion density, can take place in about $10^{-4}\ \tau$ seconds. The open grain boundaries seen on rapidly fractured specimens are in agreement with these relaxation and blunting times.

Initial Instability and Crack Propagation at the Interface

Contrary to metals at low temperatures which become more ductile as the temperature is raised, the copper-sapphire specimens in these experiments broke abruptly at increasingly lower stresses as the temperature went up. The threshold stress for brittle fracture for all the specimens was in fact about 30 MPa lower than the reported strength at room temperature of diffusion bonded copper-alumina specimens [3].

It is proposed that two diffusive processes are operating at the crack tip at the interface. Like the diffusion of metal atoms into grain boundaries to promote pore growth [1], the copper atoms can diffuse from the crack tip into the copper-sapphire interphase boundary under an applied stress to promote crack propagation. The diffusion of the copper atoms are driven in this model by a stress concentration at the crack tip that varies as $r^{-1/2}$, where r is the distance from the crack tip. If interphase boundary diffusion is sufficiently rapid, the diffusion of copper atoms away from the crack tip will elongate the crack and decrease the crack tip radius, resulting in increasingly rapid interphase boundary diffusion and crack propagation.

A second diffusion process will tend to blunt the crack tip. Since atoms on a curved surface have a higher chemical potential than those on a flat surface, the copper atoms will diffuse away from the crack tip, thus

causing its radius to increase. This diffusion will decrease the stress concentration at the crack tip and if sufficiently rapid, will offset any decrease in crack tip radius caused by the interphase boundary diffusion. In this model crack advance from the blunting is not included as it was in a model by Chuang and Rice [17]. Surface diffusion is here seen as a competitive process with interphase diffusion that serves to slow down crack advance.

In the following analysis a relation is derived between the surface diffusion coefficient D_S and the interphase boundary diffusion coefficient D_I for which the crack tip radius R remains constant. Estimated ratios of D_S/D_I are then compared at different temperatures to the ratios of the threshold stresses causing brittle fracture at these same temperatures.

Analogous to the model for a crack tip profile developed by Chuang and Rice [17], the boundary flux of atoms at the copper-sapphire interface can be written as

$$J_I = \frac{-D_I \upsilon}{kT} \frac{d\Delta\mu}{dx} \tag{12}$$

where υ is the copper surface concentration of atoms. From conservation of matter

$$\frac{dJ_I}{dx}\Big|_{x=R} = \frac{V}{\Omega} \tag{13}$$

where V is the velocity of the crack and Ω the atomic volume. The x coordinate axis runs along the sapphire surface as shown in Figure 10.

In this model a thin slice of material is considered that runs parallel to the x axis. The difference in chemical potential at the interface between the stressed and unstressed state is given by [18]

$$\Delta\mu = -T_n\Omega \tag{14}$$

where T_n is the traction along the interface given approximately by

$$T_n = \frac{1.1}{\sqrt{2}}\sigma_\infty\sqrt{\frac{c}{x}} = \frac{K}{\sqrt{2}x^{1/2}} \quad R \le x \le C \tag{15}$$

where K is $1.1\sigma_\infty\sqrt{c}$, σ_∞ is the remote applied stress, and c is the crack length. Combining equations (12) to (15) gives

$$J_I = \frac{-D_I\Omega\ \nu\ K}{2\sqrt{2}\ kT\ x^{3/2}} \quad R \le x \le C \tag{16}$$

which is the number of atoms flowing per unit length per unit time in the boundary ahead of the crack tip.

The velocity of the crack may then be written as

$$V = \frac{3\Omega^2 D_I\ \nu K}{4\sqrt{2}\ kT\ R^{5/2}} \tag{17}$$

If there is no crack blunting, the radius R decreases with time and the velocity rises quickly. If surface diffusion

is sufficiently fast to blunt the crack tip and keep R constant, V will remain constant. Otherwise, R = R(t) and V = V [R(t)].

The surface flux of atoms from the crack tip to the flat surface behind it (Figure 10) is given by [17]

$$J_s = \frac{-D_s \nu}{kT} \frac{d(\Delta\mu)}{ds} \tag{18}$$

where s is the coordinate along the crack surface and is zero behind the crack tip. The difference in chemical potential between an atom at the crack tip and on the flat surface is

$$\Delta\mu = \frac{\gamma\Omega}{R} \tag{19}$$

where γ is the metal surface energy. If the crack tip is modelled as a semicircle then the gradient in chemical potential can be approximated as

$$\frac{\Delta(\Delta\mu)}{\Delta s} = \frac{\gamma\Omega}{R} \frac{1}{\left(\frac{1}{2}\right)\frac{\pi R}{2}} = \frac{4\gamma\,\Omega}{\pi R^2} \tag{20}$$

Combining equations (18) to (20) gives

$$J_s = - \frac{4D_s\,\Omega\,\nu\gamma}{kT\,\pi\,R_2} \tag{21}$$

as the surface flux of atoms blunting the crack tip.

If J is assumed zero behind the crack tip, then the number of atoms flowing per unit area per unit time from the crack tip can be approximated by

$$\frac{\Delta J}{\Delta S} = -\frac{4D_s \Omega \nu \gamma}{kT \pi R^2} \frac{1}{-\left(\frac{1}{2}\right)\frac{\pi R}{2}} \tag{22}$$

$$= \frac{16 D_s \Omega \nu \gamma}{kT \pi^2 R^3}$$

For every unit length of crack advance δ where δ is taken as the boundary width, surface diffusion must remove $\frac{\pi R}{2\delta}$ times as many atoms that diffused to cause the crack advance to keep R constant. This condition may be written

$$\frac{dV_s}{dt} = \frac{\pi R}{2\delta} \frac{dV_I}{dt} \tag{23}$$

where dV_S/dt is the rate of volume change on the crack surface and dV_I/dt is the rate of volume change in the boundary adjacent to the crack tip.

The number of atoms per unit area per unit time flowing into the boundary at the crack tip is given by

$$\frac{dJ_I}{dx}\Big|_{x=R} = \frac{3\Omega D_I \upsilon K}{4\sqrt{2}\, kT R^{5/2}} \tag{24}$$

dV_I/dt may then be written

$$\frac{dV_I}{dt} = \Omega \delta^2 \left[\frac{3\Omega D_I \upsilon K}{4\sqrt{2}\, kT R^{5/2}}\right] \tag{25}$$

dV_S/dt may be written from equation (22) as

$$\frac{dV_s}{dt} = \Omega\,\delta^2\left[\frac{16\,D_s\,\Omega\,v\gamma}{kT\,\pi^2\,R^3}\right] \tag{26}$$

Combining equations 23, 25, and 26 gives

$$D_s = \frac{3\,\pi^2\,K\,R^{3/2}D_I}{128\,\sqrt{2}\gamma\delta} \tag{27}$$

The equation above shows that if temperature increases to increase D_I or if σ_∞ increases, D_S must increase accordingly to keep the rate of crack blunting high.

The following calculations compare the curves in Figure 2 with equation 27. Data for time to fracture versus temperature in Figure 1 predict that the transition to brittle fracture occurs at 600°C for an applied stress of 4.55 MPa. If the activation energy Q_S for surface diffusion is estimated to be 38.2 kcal $mole^{-1}$ and a preexponential factor is given a value 0.034 [19], then the surface diffusion coefficient D_S can be approximated as $9.3x10^{-12}$ m^2 s^{-1} at 600°C.

An approximation to D_I can be calculated from equation 27. With a crack tip radius of 1 μm, a stress concentration factor of 4, a copper surface energy of 1.96 J/m^2, and a boundary width of 3 Å, D_I at 600°C is $2.8x10^{-15}$ m^2 s^{-1}. In order to get the order of magnitude of D_I at different temperatures, an activation energy Q_I must be estimated. If it is assumed that the preexponential factor for D_I is the same as that for D_S, then Q_I is 52.2 kcal $mole^{-1}$.

A ratio of D_S/D_I can now be estimated at the temperatures at which actual fracture tests were done to construct Figure 2. This ratio according to equation 27 should vary according to K or σ_{crit}, the critical stress at which brittle fracture began at each temperature. In other words, for temperatures T_1 and T_2,

$$\frac{(D_s/D_I)_{T_1}}{(D_s/D_I)_{T_2}} = \frac{(\sigma_{crit})_{T_1}}{(\sigma_{crit})_{T_2}} \tag{28}$$

For the tests done in hydrogen forming gas at 800 and 750°C, the left hand side of equation 28 is 0.73 and the right hand side is 0.72. For the tests done in argon at 700 and 600°C, the two sides of equation 25 are 0.67 and 0.80 respectively. Although many estimations were done for this comparison, the decreases in critical stress at increasing temperatures are on the same order of magnitude as the changing ratios of D_S/D_I.

The low stresses at which cracks begin to propagate through the interface are in agreement with the thermodynamics of brittle fracture. Because the fracture is occurring at high temperatures, the change in free energy ΔG will contain a term for the work done by stress assisted diffusion in creating a crack of height h and length ℓ [20].

If at the crack tip the local stress σ_n causing the diffusion is $\sigma_\infty(x/R)^{1/2}$, then the work done by diffusion in the crack extension is

$$\sigma_\infty h \int_0^\ell \sqrt{\frac{x}{R}}\, dx = \frac{2\sigma_\infty h \ell^{3/2}}{3\sqrt{R}} \tag{29}$$

At low stresses the work done by the diffusion is much greater than the decrease in strain energy approximately by $\sigma_\infty^2 \ell^2 / E$, so that the change in free energy per unit crack length may be approximated as

$$\Delta G = (\gamma_c + \gamma_m)\ell - \frac{2\sigma_\infty h \ell^{3/2}}{3\sqrt{R}} \tag{30}$$

The first term in the above equation is the increase in surface energy as the crack spreads. Minimizing ΔG with respect to ℓ gives a critical crack length ℓ_c as

$$\ell_c = \frac{(\gamma_c + \gamma_m)^2 R}{\sigma_\infty^2 h^2} \tag{31}$$

Taking γ_c and γ_m for alumina and copper as 1.02 J/m^2 and 1.98 J/m^2 respectively, a crack radius of 0.5 μm, and h although unknown as 0.1 to 0.5 μm, gives a critical crack length of 2 to 50 μm for σ_∞ at 3 MPa, which is reasonable for the diameter of the specimen.

The decrease in threshold stress for the polycrystalline copper-sapphire specimens can be accounted for by including in the expression for ΔG a term for the work done in opening the crack by grain boundary sliding [21]:

$$\Delta G = (\gamma_c + \gamma_m)\ell - \frac{2\sigma_\infty h\ell^{3/2}}{3\sqrt{R}} - \tau S\ell \qquad (32)$$

where τ is the resolved shear stress along the grain boundaries and S is the sliding displacement. If Θ is the angle between the metal-ceramic interface normal and a grain boundary, then $S \sim h/\cos\Theta$ and $\tau = (\sigma_\infty/2)\sin 2\Theta$. The term τS then becomes $\sigma_\infty h \sin\Theta$, whose average with respect to Θ from 0 to $\pi/2$ is $(2/\pi)\,\sigma_\infty h$. ΔG may then be written

$$\Delta G = [\gamma_c + \gamma_m - (2/\pi)\sigma_\infty h]\ell - \frac{2\sigma_\infty h\ell^{3/2}}{3\sqrt{R}} \qquad (33)$$

Minimizing ΔG with respect to ℓ now gives

$$\ell_c = \frac{[\gamma_c + \gamma_m - (2/\pi)\sigma_\infty h]^2}{\sigma_\infty^2 h^2} \qquad (34)$$

The threshold stress for polycrystalline copper-sapphire specimens at 750°C was about 1.3 MPa, which when substituted in the above equation with the same numbers as before and h as 0.1 to 0.5 μm, gives ℓ_c 3 to 86 μm. The work done by sliding boundaries therefore makes it thermodynamically feasible for a crack to reach a critical length at just a slightly lower stress.

Conclusions

Pore nucleation and growth leading to fracture at metal-ceramic interfaces occurs only under specific experimental conditions. For a set applied stress it

occurs at lower temperatures and at a constant temperature it occurs at lower stresses. At both higher stresses and temperatures brittle fracture becomes faster than pore growth. The inhomogeneous distribution of pores near the transition region along with the small critical size of the pores in comparison with the applied stress suggests that the nucleation and growth of the pores is governed by stress concentrations.

The decrease in critical stress with increasing temperature is too large to be accounted for by the decrease in the metal and ceramic surface energies that arise when a crack propagates in a brittle manner. Instead the ratio of surface to interface diffusion coefficients has been shown to decrease with temperature relative to the ratio itself by the roughly the same amount as critical stress decreases relative to itself. Instability and the mode of fracture at high temperatures therefore seems to be governed by processes that depend exponentially on temperature.

References

1. R. Raj and M.F. Ashby. Acta. Metall. 23 653 (1975).

2. R. Raj. Acta. Metall. 26 341 (1978).

3. J.T. Klomp. Science of Ceramics 5 501 (1970).

4. B.J. Dalgleish, E.B. Slamovich and A.G. Evans. J. Amer. Ceram. Soc. 68 [11] 575 (1985).

5. V. Sklenicka, I. Saxl, and J. Cadek. Res. Mech. 1 301 (1980).

6. A. Magata and I.W. Hall. J. Mater. Sci. 24 1959.

7. T.S. Oh, J. Rödel, R.M. Cannon, and R.O. Ritchie. Acta. Metall. 36 [8] 2083 (1988).

8. P.A. Mataga, Acta. Metall. 37 [12] 3349 (1989).

9. G.E. Rhead, Acta Metall. 13, 323 (1965).

10. C.M. Kennefick and R. Raj, Acta Metall. 2947 (1989).

11. R.M. Pilliar and J. Nutting. Philos. Mag. 16 181 (1967).

12. R. Raj. Acta. Metall. 26 995 (1978).

13. P.J. Clemm and J.C. Fisher, Acta. Metall. 3 70 (1955).

14. M.H. Yoo and H. Trinkhaus, Metall. Trans. A, 14A 547 (1983).

15. A.G. Evans, J.R. Rice, and J.P. Hirth, J. Amer. Ceram. Soc. 63 [7-8] 368 (1980).

16. R. Raj, Metall. Trans. A 6A 1499 (1975).

17. J. Chuang and J. R. Rice. Acta Metall. 21 1625 (1973).

18. C. Herring. J. Appl. Phys. 21 437 (1950).

19. G. Neuman and G. M. Neuman. Surface Self Diffusion of Metals. Diffusion Information Center (1972).

20. R.N. Stevens and R. Dutton, Mater. Sci. and Engin. 8 220 (1971).

21. H.E. Evans, Philos. Mag. 23 1101 (1971).

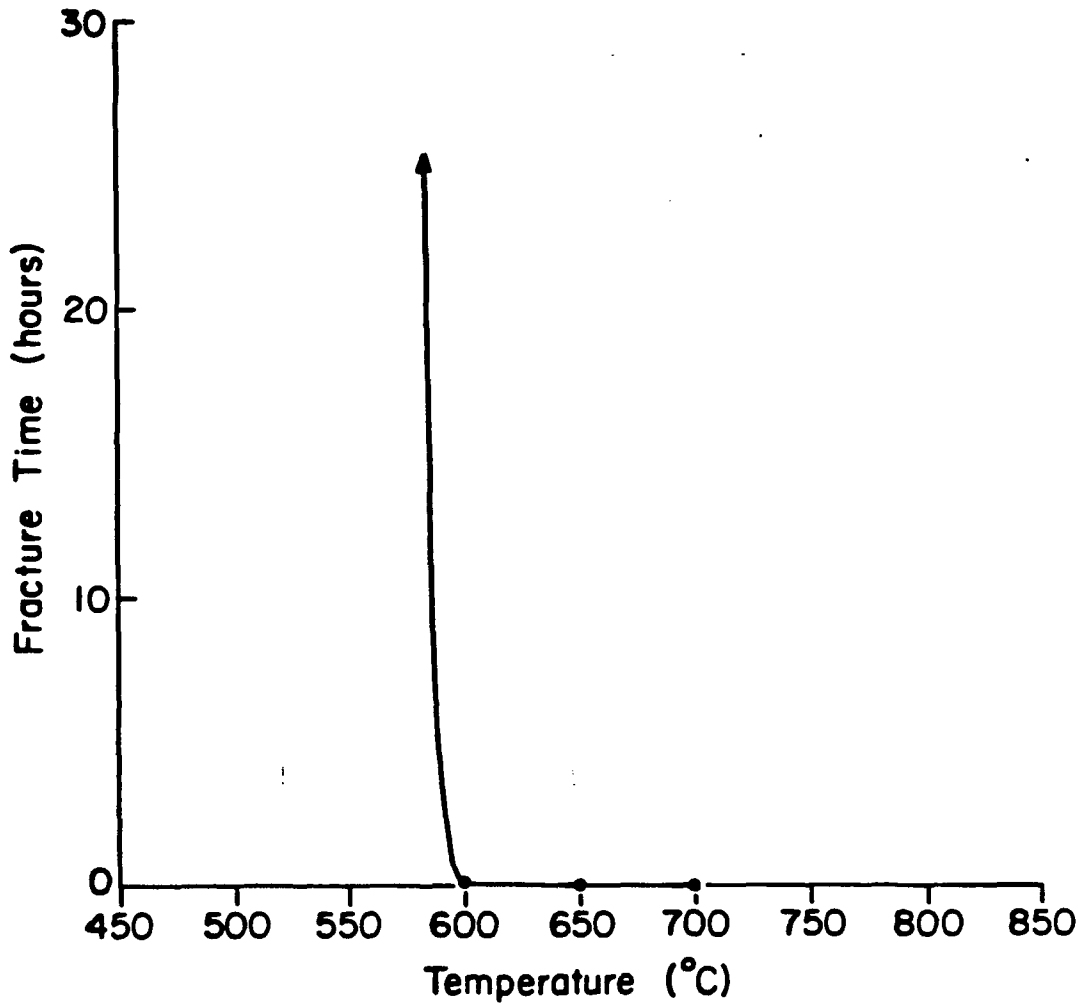

Figure 1. Time to fracture versus temperature for single crystal copper-sapphire specimens under a stress of 4.55 MPa.

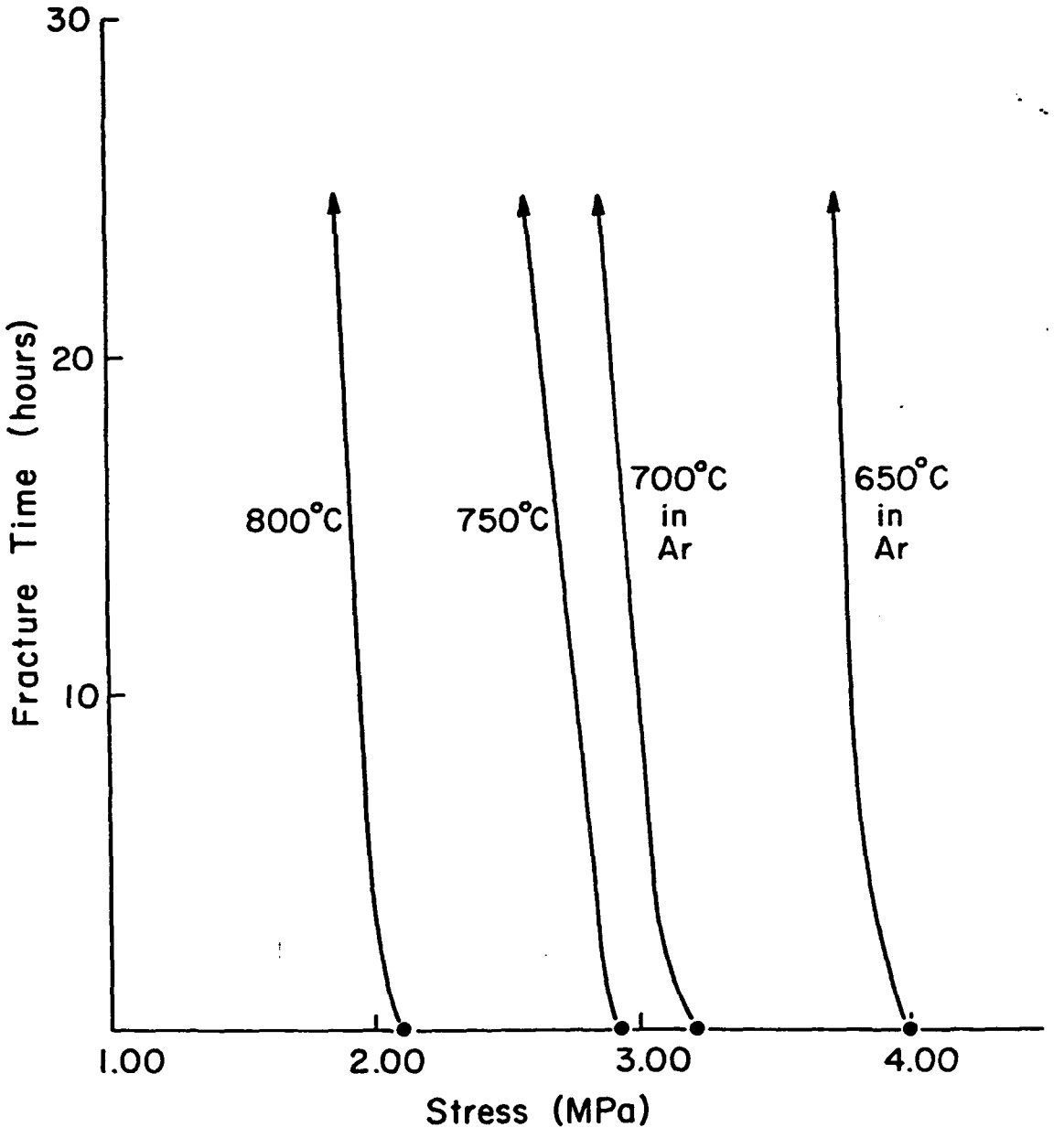

Figure 2. Time to fracture versus stress for single crystal copper-sapphire specimens tested at various temperatures. The tests were done in 86% argon/14% hydrogen unless argon is indicated otherwise.

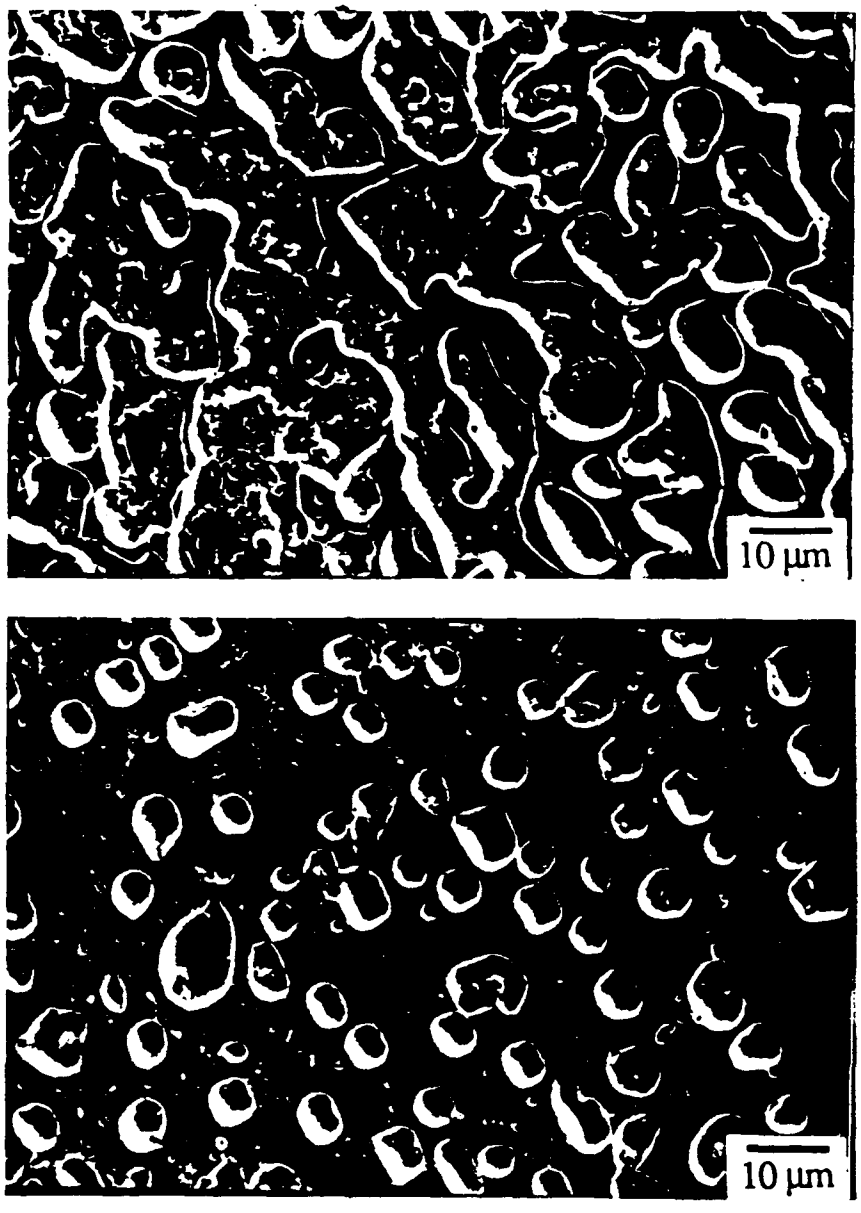

Figure 3. Pores on the copper surface of a single crystal copper-sapphire specimen held under a tensile stress of 2.64 MPa at 700°C for 48 hours. The upper photograph was taken near the edge of the specimen whereas the lower was taken closer to the middle of the same specimen.

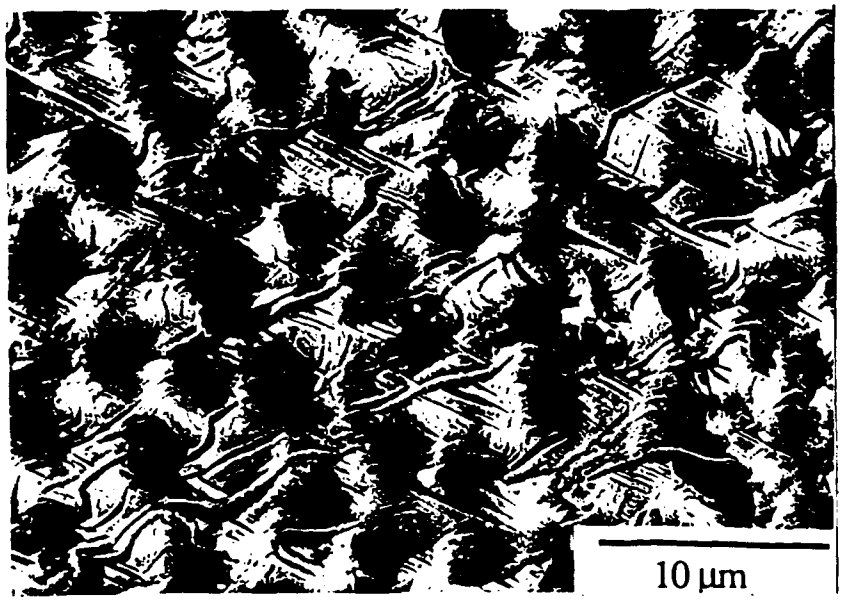

Figure 4. Slip bands and striations on the copper surface of a single crystal copper-sapphire specimen which fractured in 30 minutes at 600°C under a stress of 4.55 MPa.

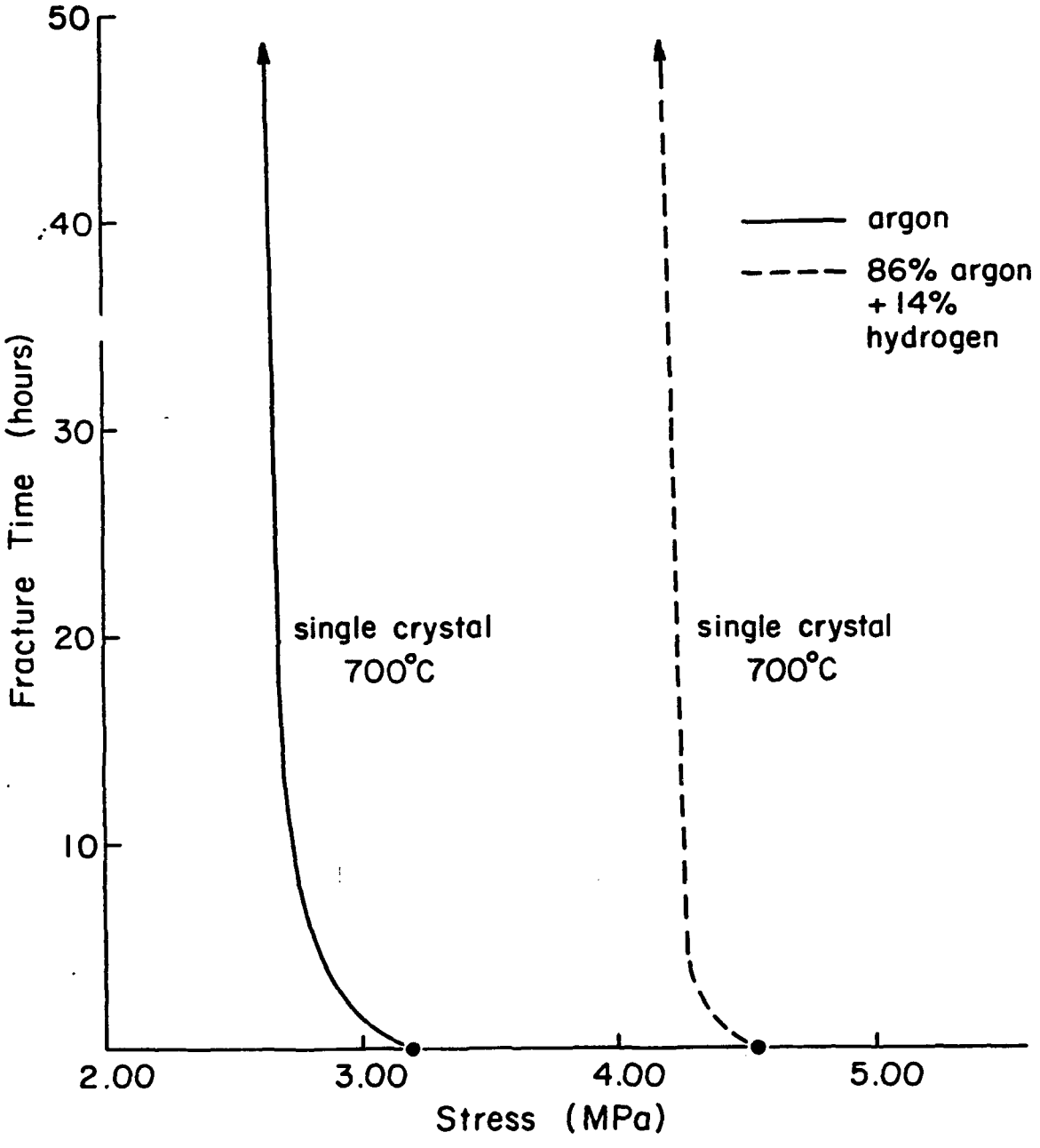

Figure 5. The difference in threshold stress for single crystal copper-sapphire specimens tested at 700°C in argon and 86% argon/14% hydrogen.

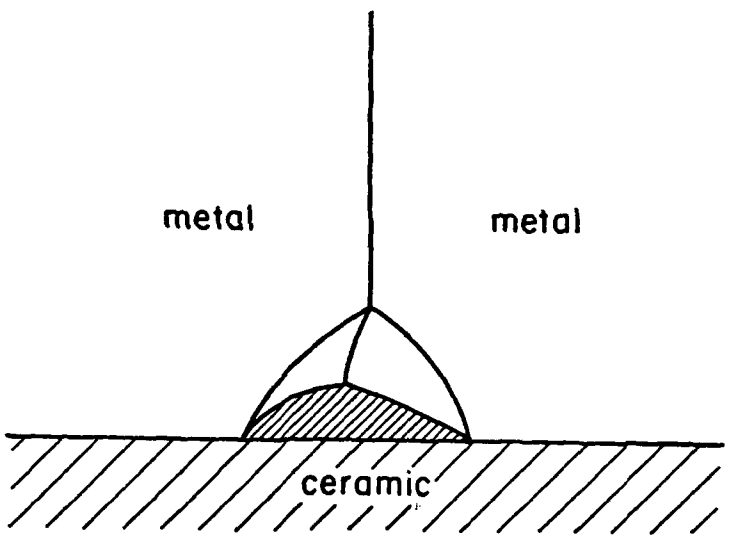

Figure 6. A pore at the intersection of a metal two-grain junction with a ceramic.

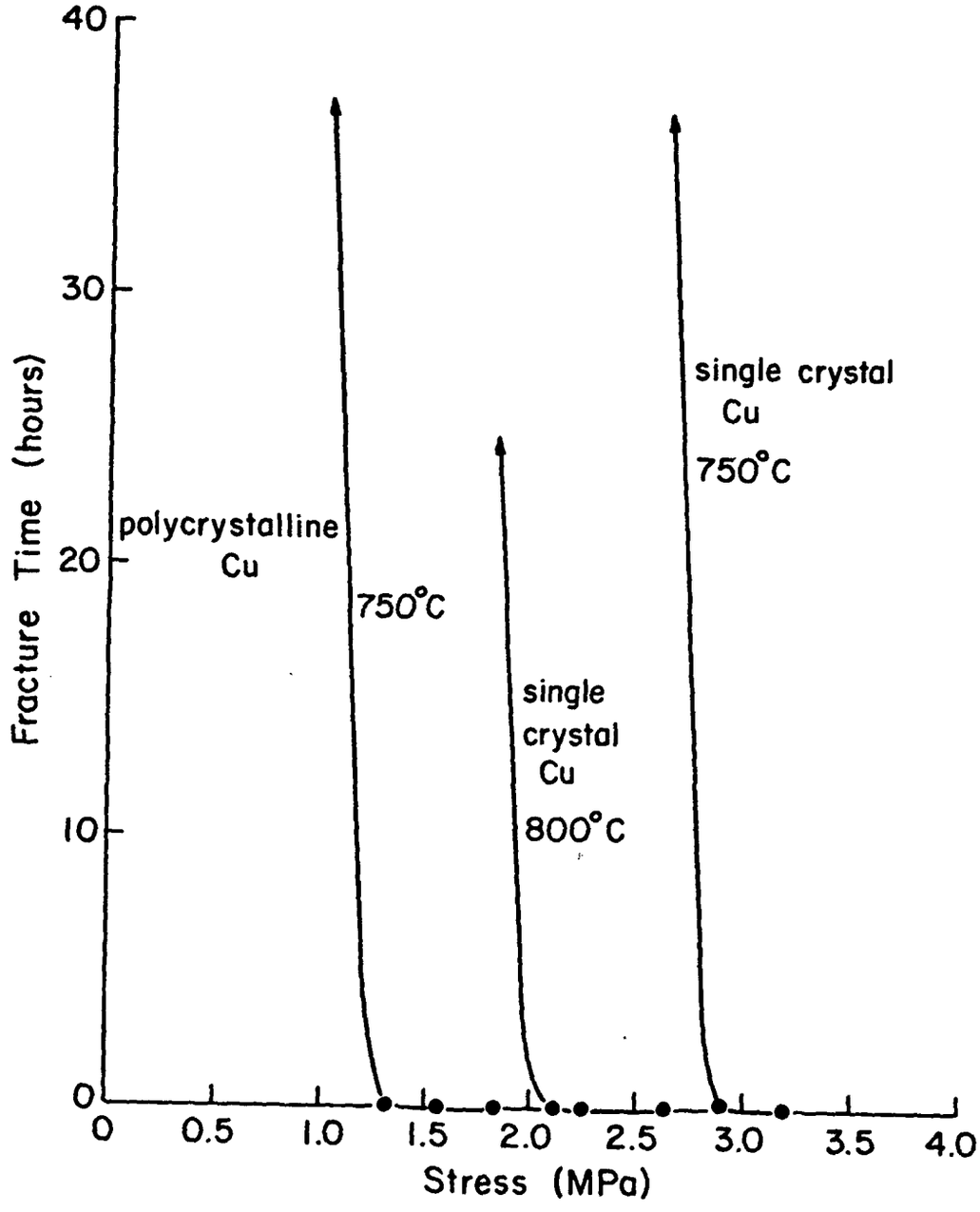

Figure 7. Comparison of the fracture time versus stress between single crystal and polycrystalline copper-sapphire interfaces.

Figure 8. Pores at a polycrystalline copper-sapphire interface after being held 37 hours at 750°C under a tensile stress of 1.02 MPa.

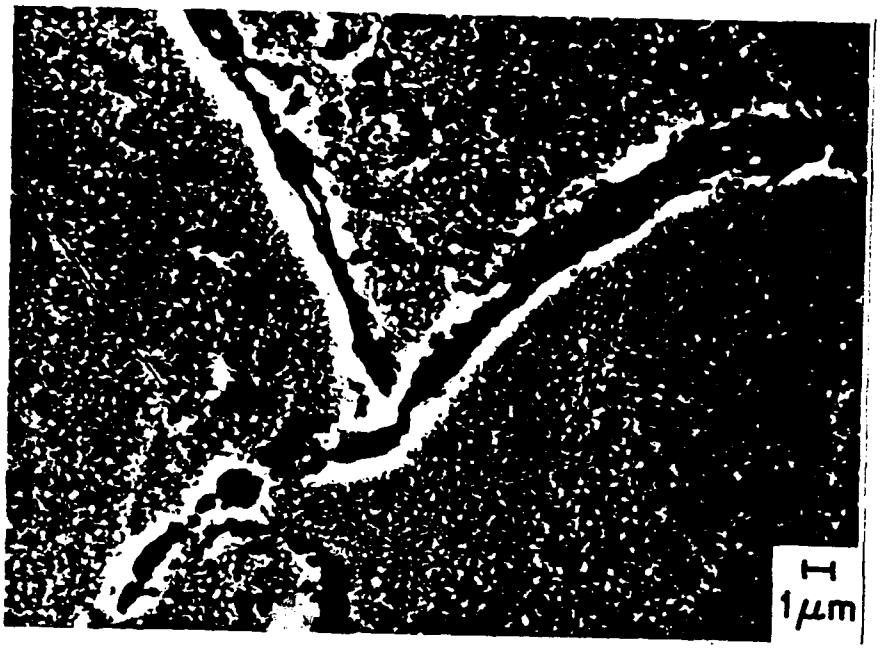

Figure 9. Grain boundaries on a copper surface from a polycrystalline copper-sapphire specimen that fractured in 5 to 10 seconds at 750°C under a tensile stress of 2.64 Mpa.

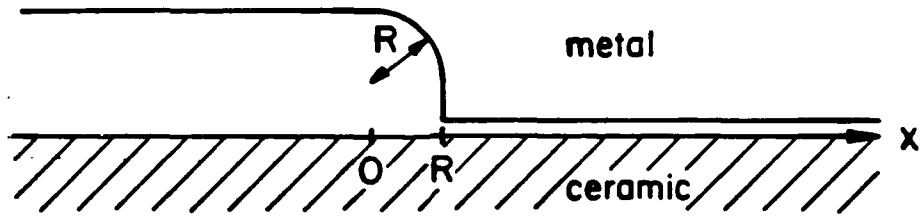

Figure 10. The crack tip profile at the copper-sapphire interface.

Appendix C

Strain Rate Dependent Sliding of a Metal Ceramic Interface at High Temperatures

V. C. Jobin and R. Raj

to be submitted for publication in Spring 1991

Strain-rate Dependent Sliding of a Metal-Ceramic Interface at High Temperatures

Valérie C. Jobin

Department of Materials Science and Engineering

Cornell University, Ithaca, NY 14853

Rishi Raj

Department of Materials Science and Engineering

Cornell University, Ithaca, NY 14853

S. Leigh Phoenix

Department of Theoretical and Applied Mechanics

Cornell University, Ithaca, NY 14853

Key words: Sliding, metal-ceramic interface, high temperature, deformation mechanism, activation energy

Abstract

Rate-dependent constitutive equations for local shear deformation at or very near a metal-ceramic interface were measured by the periodic cracking technique. Experiments with copper-silica interfaces revealed two regimes of behavior.

In the low strain-rates/high temperatures regime, a strong strain-rate dependency of the characteristic parameter of the system, that is the normalized average steady-state crack-spacing, was observed. A power law fit between the shear deformation rate, or sliding-rate, and the local shear stress was used and the stress exponent n was found to equal 1 ± 0.04 in this regime. In the regime corresponding to high strain-rates/high temperatures and low temperatures, this characteristic parameter was found to be independent of strain-rate.

These results, when analized in terms of the global mechanisms of deformation in crystalline materials, lead to the following interesting ideas: (a) the diffusional mechanism of creep can be applied to metal-ceramic interfaces by assuming that sliding at an undulating shape of the interface is accommodated by interfacial diffusional transport in the metal, (b) the power-law creep mechanism is not observed for deformation near the interface because the width of the deformation zone near the interface is smaller than the characteristic subgrain size required in power-law creep, and (c) at high strain-rates/high temperatures and low temperatures, sliding at the interface can occur by slip in the metal except that, for the copper-silica system, the stress required for such slip is much greater than the intrinsic Peierls stress for bulk copper because the interface is not atomically planar. A rigorous analysis of the diffusional mechanism is presented.

Introduction

Metal-ceramic composites have received vast attention in the past decade due to their superiority over resin matrix composites with regard to mechanical properties such as tranverse strength and shear properties and, more importantly, due to their high temperature capabilities [1]. The achievement of their optimum potential depends not only on the properties of the bulk constituents which are easy to assess, but also on the more complex properties of the interface. Therefore, gaining a fundamental understanding of the metal-ceramic interfacial phenomena has become a crucial issue [2, 3, 4] since it will promote design of improved composites through tailored interfaces.

From a mechanical point of view, interest focuses on determining the tensile and shear strengths of the interface. Presently, few experimental techniques yielding strength data are available [5, 6, 7]. The technique used in this study, the periodic cracking of a thin brittle film on a ductile substrate [8, 9, 10], allows low and high temperature measurements of the ultimate shear strength of a metal-ceramic interface [11] and can provide a wealth of quantitative and qualitative data with regard to the deformation mechanisms at a metal-ceramic interface. This method has many similarities with the single-filament-composite test [12] and was presented in detail by previous authors [11].

In the present study, our goal is to identify and characterize the high temperature deformation mechanisms at a metal-ceramic interface which is subjected to shear loading and also to compare the active mechanisms at the interface with those active in the bulk metal. Constitutive equations are developed.

Experimental procedure

Experimental technique

Figure 1 is a schematic of the experimental technique. When the metal substrate is pulled in uniaxial tension at a constant strain-rate, tensile stresses are transmitted directly from the substrate to the thin ceramic film via the interface. At strains close to the elastic limit of the film and corresponding to plastic deformation in the metal, a system of cracks parallel to each-other and perpendicular to the tension axis develops in the film as seen in figure 1. Due to the difference in tensile behavior of the two deforming materials, shear stresses arise at the interface between adjacent cracks.

The crack- density defined as the inverse of the crack-spacing $1/\lambda$ shows a sigmoidal behavior when plotted as a function of the increasing plastic strain in the metal substrate ϵ (see figure 1). The sharp increase of the crack-density occurs when the applied strain equals the fracture strain ϵ_f of the ceramic film. ϵ_f includes the contribution from the thermal strain due to the thermal expansion coefficient mismatch between the film and the substrate. The tensile strength of the film $\hat{\sigma}$ is then given by:

$$\hat{\sigma} = \epsilon_f E_c \tag{1}$$

where E_c is the Young's modulus of the ceramic film.

Eventually, the crack-density reaches a saturation level when the elastic deformation in the film is maximum. A steady-state regime is then reached. The average steady-state crack-spacing $\bar{\lambda}$ is characteristic of the ultimate shear strength of the metal-ceramic interface and depends on external parameters such as temperature and strain-rate.

In the steady-state regime, if no debonding of the ceramic strips still attached to the substrate is to occur, another mechanism accommodating further stretching

of the interfacial region must become dominant. Sliding at the interface is such a deformation accommodation mechanism and is studied in detail in this paper for a regime of high temperatures and low strain-rates.

Materials

Pure copper (99.9%) tensile specimens coated with thin films of silica SiO_2 were used as a metal-ceramic model system. A full description and characterization of the films obtained through the sol-gel process can be obtained in reference [11]. The density of the films was found to equal $(95 \pm 1)\%$. The coated copper specimens had a gauge length of 1 cm and were pulled uniaxially in a constant strain-rate tensile machine[1]. equipped with a high temperature furnace[2]. Tensile tests were performed in argon at different sets of temperatures and strain-rates ranging respectively from room temperature to 550°C and from 1.7×10^{-3}/s to 1.6×10^{-5}/s.

Film thicknesses and crack-spacings were measured with a microprobe[3].

Model of sliding at the interface

Stress consideration

Figure 2(a) shows a portion of the film in cross-section located between two cracks A and B a distance λ apart. The crack-density is now constant (steady-state regime). This means that the in-plane stress σ in the film can not build up to a value high enough to equal the film tensile strength $\hat{\sigma}$. In some cases however, σ equals $\hat{\sigma}$ in the middle section of the ceramic strip when the distance λ equals the upper limit of the final crack-spacing distribution [11]. The ceramic film strip can be viewed as a rigid body on the plastically deforming metal substrate. Assuming the constant strain-rate

[1]Instron, model 1137.
[2]Centorr, model M-60.
[3]Jeol, model 733.

to be uniform throughout the substrate, the relative sliding-rate $\dot{u}$ which represents the relative displacement δu of the copper substrate with respect to the silica film per time δt should be maximum at $x = 0$ and $x = \lambda$ and antisymmetric. In the same way as one begins by assuming a strain field compatible with the applied displacements in large-deformation plasticity problems, we assume here that the sliding-rate $\dot{u}$ is a linear function of the position x fulfilling the previous requirements. Such a rate distribution is the most compatible with the concepts of steady-state regime and large deformations (the strains attained in the steady-state regime are greater than 5%). Therefore,

$$\dot{u}(x) = a_0(x - \lambda/2) \tag{2}$$

where a_0 is a constant (see figure 2(b)).

In the next equation, we relate the amplitude of the local shear stress at the interface τ to the amplitude of the relative sliding rate $\dot{u}$ through a power- law relationship of the general form

$$\dot{u}(x) = -\alpha(T)\tau^n(x) \tag{3}$$

where α is a positive constant which depends on the absolute temperature. The sliding-rate $\dot{u}$ plays a similar role for characterizing deformation at a metal-ceramic interface as the one played by the shear strain-rate $\dot{\gamma}$ used in the rate-equations of bulk polycrystalline materials [13].

From equation 3, $\tau(x)$ is maximum at the edges of the strip and equal to zero at its center which agrees with the basic features recommended for the interfacial shear stress distribution. In reality, the very details of such a distribution are not well-known and several approximations were suggested in the literature for small deformations at the interface [14, 15].

We can consider only the left half of the ceramic strip that is from $x = 0$ to $x = \lambda/2$ due to the symmetry of the problem. We know that the shear stress distribution $\tau(x)$ should be antisymmetric to fulfill the requirement that the shear stress integrated over the distance $x = 0$ to $x = \lambda$ be equal to zero due to the free-body equilibrium condition applied to the whole section of the film AB. The symmetric in-plane stress in the film σ, is assumed to be uniform through the thickness of the film and depends on the position x. A free-body equilibrium condition applied in the film at different values of x leads to the equation

$$\sigma(x) = \frac{1}{t}\int_o^x \tau(y)dy \tag{4}$$

where t is the thickness of the film.

Equations 2 and 3 combined with 4 yield the position-dependency of σ. The maximum value of $\sigma(x)$ occurs when $x = \lambda/2$. This maximum value is equal to the film tensile strength $\hat{\sigma}$ when the distance λ is equal to the maximum crack-spacing denoted as λ_m which is obtained in the steady-state crack-spacing distribution as mentioned earlier:

$$\hat{\sigma} = \frac{n}{n+1}\frac{1}{t}\left(\frac{a_0}{\alpha}\right)^{\frac{1}{n}}\left(\frac{\lambda_m}{2}\right)^{1+\frac{1}{n}}. \tag{5}$$

The maximum shear stress acting at the interface $\hat{\tau}$ is reached when $x = 0$ such that

$$\hat{\tau} = \left(\frac{-a_0}{\alpha}\right)^{\frac{1}{n}} \tag{6}$$

and

$$\hat{\tau} = \left(\frac{a_0}{\alpha}\right)^{1/n}\left(\frac{\lambda_m}{2}\right)^{\frac{1}{n}}. \tag{7}$$

Equations 5 and 7 lead to

$$\hat{\sigma} = \frac{\lambda_m}{2t}\frac{n}{n+1}\hat{\tau}. \tag{8}$$

Due to the statistical nature of brittle cracking in the ceramic film, an improved version of equation 8 can be obtained when the distance λ_m is replaced by the average steady-state crack-spacing $\bar{\lambda}$ such that

$$\hat{\tau} = \frac{2(n+1)}{n} \frac{t}{\bar{\lambda}} \hat{\sigma}. \tag{9}$$

Strain consideration

Figure 3(a) represents an initial length L_0 of the film before stretching starts. L_0 can stretch elastically by an amount $\epsilon_f L_0$ before cracking occurs (see figures 3(b) and 3(c)). For simplification, we assume that cracks initiate and propagate in the film within a very sharp region of strains which can eventually be represented by the single value ϵ_f. When the cracking process is over, that is after m cracks have formed in the film, interface sliding becomes dominant and results in a steady-state opening of the cracks (see figure 3(d)). $\bar{w}$ represents the average crack-opening amplitude at time t. The previous statements lead to the following equations:

$$L_0 = \frac{(m+1)\bar{\lambda}}{(1+\epsilon_f)} \tag{10}$$

and

$$L = (m+1)\bar{\lambda} + m\bar{w}. \tag{11}$$

L_0 and m are sufficiently large that use of the average values $\bar{\lambda}$ and $\bar{w}$ is meaningful. The plastic strain ϵ in the steady-state regime can be reasonably approximated by

$$\epsilon = \frac{L - L_0}{L_0} \tag{12}$$

Inserting equations 10 and 11 in 12, we obtain

$$\epsilon = \epsilon_f + \frac{m}{m+1}(1+\epsilon_f)\frac{\bar{w}}{\bar{\lambda}} \tag{13}$$

The only parameter on the right side of the above equation which depends on time as strain increases is $\bar{w}$. Equation 13 differentiated with respect to time yields the relationship

$$\dot{\epsilon} = \frac{m}{m+1}(1+\epsilon_f)\frac{\dot{\bar{w}}}{\bar{\lambda}}, \tag{14}$$

and m being very large, $\frac{m}{m+1} \approx 1$, so that

$$\dot{\epsilon} = (1+\epsilon_f)\frac{\dot{\bar{w}}}{\bar{\lambda}}. \tag{15}$$

Equation 15 establishes the relationship between the applied constant strain-rate $\dot{\epsilon}$ and the steady-state crack-opening rate $\dot{\bar{w}}$.

Continuity of deformation

A principle of continuity of the rate at which the interface accommodates deformation can be applied at point A on figure 2(a). At this point, from the substrate perspective, the amplitude of the interface sliding- rate which is maximum in A and the amplitude of the crack-opening rate should be equal

$$-\dot{u}(0) = \dot{\bar{w}}. \tag{16}$$

Equations 6, 15 and 16 combined together yield

$$\hat{\tau} = \left(\frac{\dot{\epsilon}\bar{\lambda}}{\alpha(1+\epsilon_f)}\right)^{\frac{1}{n}} \tag{17}$$

Finally, a comparison of equation 9 to 17 leads to

$$t/\bar{\lambda} = f(n,T)(\dot{\epsilon}\bar{\lambda})^{\frac{1}{n}} \tag{18}$$

where

$$f(n,T) = \frac{n}{2(n+1)}\frac{1}{\hat{\sigma}}\left(\alpha(T)(1+\epsilon_f)\right)^{-\frac{1}{n}} \tag{19}$$

Equation 18 states that the ratio $t/\bar{\lambda}$ is proportional to the quantity $(\dot{\epsilon}\bar{\lambda})^{\frac{1}{n}}$ at a constant temperature. The parameters t and $\bar{\lambda}$ can be measured experimentally at different temperatures and strain-rates. Therefore, our experimental results can be used to determine the exponent n and the regime of temperatures and strain-rates where equation 3 applies.

Results

We measured the average steady-state crack-spacing $\bar{\lambda}$ in the silica films at different decreasing strain-rates at four temperatures ranging from room temperature to 500°C. Experimental results are summarized in table 1 where calculations of the ratio $\bar{\lambda}/t$ are also displayed.

Figure 4 represents the variations of the average steady-state crack-spacing normalized to the film thickness $\bar{\lambda}/t$ versus strain-rate at 20°C, 100°C, 300°C and 500°C. Two distinct regimes of temperatures and strain-rates reflecting different trends in interface behavior can be observed.

The first one groups the low temperatures (below 100°C) and the high temperatures (above 300°C)/high strain-rates (above $\dot{\epsilon}_s = 1.7 \times 10^{-4}$/s) domains. In this regime, the ratio $\bar{\lambda}/t$ is found to be roughly constant, that is independent of strain-rate at a given temperature. According to equation 18, this means that the exponent n is infinite in this regime. In such a case, equation 19 states that the temperature effect contained in $\alpha(T)$ is suppressed. This contradicts the tendency observed on figure 4 which shows explicitly that at a given strain-rate, the ratio $\bar{\lambda}/t$ is a function of temperature. For this regime of temperatures and strain-rates, sliding at the interface can occur by slip in the metal but equation 3 does not apply. Further investigation of this behaviour can be obtained in reference [16].

The second domain on which our interest will focus, is the high temperatures (above 300°C)/low strain-rates (below $\dot{\epsilon}_s$) regime. A sharp increase of $\bar{\lambda}/t$ with decreasing strain-rate for strain-rates below $\dot{\epsilon}_s$ is noticeable for the two elevated temperatures 300°C and 500°C. Typical micrographs of cracked silica films strained at 500°C and various strain-rates are shown in the steady-state regime on figure 5. The increase of the crack-spacing with decreasing strain-rate can be observed.

We have plotted the experimental results obtained in this second domain in a different manner. According to equation 18, the exponent n can be obtained from a plot $\ln(t/\bar{\lambda})$ versus $\ln(\dot{\epsilon}\bar{\lambda})$ at a given elevated temperature since these two quantities should be linked linearly, the slope of the line being equal to $1/n$. Figure 6 represents two such plots at 300°C and 500°C. In both cases, a linear relationship was obtained and the slope $1/n$ was found to equal 0.975 at 300°C and 1.041 at 500°C. Hence, n is approximately equal to 1

$$n = 1 \pm 0.04 \tag{20}$$

This result is more obvious when the ratio $\dot{\epsilon}\bar{\lambda}^2/t$ is plotted versus strain-rate as shown on figure 7. Equation 18 states that this ratio should become constant. This tendency can be observed on the plot for strains below $\dot{\epsilon}_s$.

Consequently, according to equation 3, the intensity of the sliding-rate is directly proportional to the intensity of the local shear stress

$$\dot{u} = -\alpha(T)\tau \tag{21}$$

Discussion

A linear relationship between the sliding-rate $\dot{u}$ and the local shear stress τ is characteristic of some of the equations derived by Raj and Ashby [17] in their extensive

work on grain-boundary sliding. In this regime of high temperatures and low strain-rates, sliding at the copper-silica interface is very likely to be diffusion-accommodated with the diffusional flow being limited to the copper-silica boundary. The importance of this type of accommodation for boundary sliding was demonstrated in a previous study [18]. Grain-boundary diffusion is favored in our system by the presence of shear stresses across the interface which generate a local distribution of normal stress at the non-planar boundary. This distribution, in turn, sets up a diffusive flow of copper atoms from regions of the boundary in compression to those in tension.

The work of the previous authors [17] can be extended and adapted to a boundary between a copper grain and a rigid strip of amorphous silica in the case of diffusion-accommodated sliding where grain-boundary diffusion prevails. The microscopic geometry of the non-planar copper-silica interface can be represented by a sine-wave boundary which is often a good approximation for a boundary shape (see figure 8). Under such conditions, the expression of the coefficient $\alpha(T)$ was derived by the previous authors for the two-dimensional problem such that

$$\alpha(T) = 8\frac{\Omega}{h^2}\frac{\delta D_B}{kT} \tag{22}$$

where Ω is the atomic volume of copper, kT is the Boltzmann's constant times the absolute temperature, δ is the thickness of the boundary diffusion path, D_B is the grain- boundary diffusion coefficient and h is the boundary height.

The product δD_B depends on T according to

$$\delta D_B = \beta \exp\left(-\frac{Q_B}{RT}\right) \tag{23}$$

where β is a constant representative of the copper-silica couple and Q_B is the activation energy of the copper-silica grain-boundary diffusion coefficient expressed in j/mol.

Equations 22 and 23 inserted in 18 with $n = 1$ yield

$$\frac{t}{\bar{\lambda}} = (\dot{\epsilon}\bar{\lambda}) \left(\frac{h^2 kT}{32\beta\Omega(1+\epsilon_f)\hat{\sigma}} \right) \exp\left(\frac{Q_B}{RT}\right) \tag{24}$$

Rearranging the above equation and taking the logarithm of its both sides, we obtain

$$\ln\left(\frac{\dot{\epsilon}\bar{\lambda}^2}{t}\right) = -\frac{Q_B}{R}\frac{1}{T} + \ln\left(\frac{1}{T}\right) + \kappa_0 \tag{25}$$

where

$$\kappa_0 = \ln\left(\frac{32\beta\Omega\hat{\sigma}(1+\epsilon_f)}{kh^2}\right) \tag{26}$$

is independent of T.

It can be observed experimentally [16] that the fracture strain ϵ_f and thus the film strength $\hat{\sigma}$ are temperature-independent constants.

Using our experimental results, an estimate of the activation energy Q_B for the copper-silica system can be obtained. Table 2 displays average experimental values of the quantity $\ln(\dot{\epsilon}\bar{\lambda}^2/t)$ measured at four elevated temperatures ranging from 300°C to 550°C. A plot $\ln(\dot{\epsilon}\bar{\lambda}^2/t)$ versus the inverse of the absolute temperature $1/T$ is represented on figure 9. The vertical bars represent ranges of experimental values. A curve of the type $\ln(\dot{\epsilon}\bar{\lambda}^2/t) = -a(1/T) + \ln(1/T) + b$ was fit through our experimental values. The curve, which in this region of temperatures is almost a straight line, is shown on figure 9. The value of the coefficient a was found to equal 4980. Hence, Q_B = 41.4 kJ/mol for the couple Cu/SiO_2. We estimated the precision on Q_B to be ±10%. For comparison, Q_B for grain-boundary diffusion at a Cu/Cu boundary is equal to 124 kJ/mol [19]. It should not be concluded too hastily that diffusion at a copper/silica boundary is faster than at a copper/copper boundary. In the process of estimating the activation energy Q_B, simplifying assumptions were made in the model and experimental error due partly to the statistical nature of brittle cracking could not be avoided. Moreover, little is known about the constant β of equation

23 and other intrinsic factors can play a very significant role in the determination of Q_B such as the interaction with the interface of dislocations nucleated in the plastically-deforming copper substrate or the presence of small amounts of impurities segregated at the copper-silica boundary. However, the order of magnitude of the activation energy Q_{Cu/SiO_2} thus calculated is excellent. It should also be mentioned that diffusion data for metal-ceramic systems is missing dramatically in the literature which prevents us to compare our value of Q_{Cu/SiO_2} with other values.

Finally, the periodic cracking technique performed at high temperatures and low strain-rates appears to be a very satisfying method to yield comparative values of grain-boundary diffusion activation energies for metal-ceramic couples which exhibit the same high temperature behavior as the copper-silica system.

Conclusions

The periodic cracking of a thin ceramic film on a thick metal substrate has proved to be a very convenient technique to study the high temperature behavior of a metal-ceramic interface deformed at various strain-rates.

Experiments performed on a copper-silica model system showed that interface sliding was an active deformation accommodation mechanism in response to high strains and shear stresses. A linear relationship between the sliding-rate and the local shear stress was obtained in a regime of high temperatures and low strain-rates. Assuming that sliding at an undulating shape of the interface is accommodated by interfacial diffusional transport in the metal, this study showed that the diffusional mechanism of creep can be applied to certain metal-ceramic interfaces. On the other hand, a power-low creep type mechanism near the interface which would correspond to a value of the exponent n ranging typically between 3 and 8 in equation 3 was not observed. This can be attributed to the size of the width of the deformation zone near

the interface which is smaller than the characteristic subgrain size (typically 1-3 μm) required in power-law creep.

It appears that deformation mechanisms of polycrystalline materials which can occur in a two-dimensional space like dislocation motion along slip planes or diffusional flow (high temperature creep), can be applied in a similar form to characterize deformation at or near a metal-ceramic interface. A deformation mechanism like power-law creep which basically requires a three-dimensional space to be effective is not an active mechanism at such interfaces.

References

[1] F.D. Lemkey, A.G. Evans, S. Fishman, and J. Strife, editors. *High temperature/high performance composites*, MRS Symposium Proceedings, 1988.

[2] A.K. Dhingra and S.G. Fishman, editors. *Interfaces in metal-matrix composites*, Metallurgical Society, Warrendale, Pa, 1986.

[3] R. Raj and S.L. Sass, editors. *Interface science and engineering '87*, Journal de Physique–Tome 49, 1988.

[4] J.A. Pask and A.G. Evans, editors. *Surfaces and interfaces in ceramic and ceramic-metal systems*, Plenum Press–New-York, 1981.

[5] V. Gupta. PhD thesis, Department of Mechanical Engineering–MIT, 1990.

[6] C.J. Yang, S.M. Jeng, and J.M. Yang. Interfacial properties measurement for SiC fiber- reinforced titanium alloy composites. *Scripta Metallurgica*, 24:469–474, 1990.

[7] J.I. Eldridge and P.K. Brinkley. Investigation of interfacial shear strength in a SiC fiber/Ti – 24Al – 11Nb composite by a fiber push-out technique. *Journal of Materials Science Letters*, 8:1451–1454, 1989.

[8] M.S. Hu and A.G. Evans. The cracking and decohesion of thin films on ductile substrates. *Acta Metallurgica*, 37:917–925, 1989.

[9] G. Gille and K. Wetzig. Investigations on mechanical behaviour of brittle wear-resistant coatings–1: experimental results. *Thin Solid Films*, 110:37–54, 1983.

[10] R. Jarvinen, T. Mantyla, and P. Kettunen. Improved adhesion between a sputtered alumina coating and a copper substrate. *Thin Solid Films*, 114:311–317, 1984.

[11] D.C. Agrawal and R. Raj. Measurement of the ultimate shear strength of a metal/ceramic interface. *Acta Metallurgica*, 37:1265–1270, 1989.

[12] A.N. Netravali, R.B. Henstenburg, S.L. Phoenix, and P. Schwartz. Interfacial shear strength studies using the single- filament-composite test. part 1: experiments on graphite fibers in epoxy. *Polymer Composites*, 10:226–241, 1989.

[13] H.J. Frost. *Deformation mechanism maps.* PhD thesis, Division of Engineering and Applied Physics, Harvard University, Cambridge, Massachusetts, 1974.

[14] W.R. Tyson and G.J. Davies. A photoelastic study of the shear stresses associated with the transfer of stress during fiber reinforcement. *British Journal of Applied Physics*, 16:199, 1965.

[15] A. Kelly. *Strong Solids.* Clarendon Press, Oxford, 1966.

[16] V. Jobin. *Deformation mechanisms at a metal-ceramic interface.* Master's thesis, Department of Materials Science and Engineering, Cornell University,Ithaca,NY, 1990.

[17] R. Raj and M.F. Ashby. On grain-boundary sliding and diffusional creep. *Metallurgical Transactions*, 2:1113–1127, 1971.

[18] R. Raj and M.F. Ashby. Grain-boundary sliding and the effect of particles on its rate. *Metallurgical Transactions*, 3:1937–1942, 1972.

[19] R.C. Koeller and R. Raj. Diffusional relaxation of stress concentration at second phase particles. *Acta metallurgica*, 26:1551–1558, 1978.

Figure 1: (a) Illustration of the experimental technique. (b) A schematic of the increase in crack-density in the ceramic film with applied strain in the metal substrate.

Figure 2: (a) The copper-silica system in cross-section. (b) The steady-state sliding-rate $\dot{u}$ as a function of x.

Figure 3: Behaviour of the interfacial region with increasing applied strain. (a) An unstretched portion of the film of initial length L_0. (b) The same portion stretched elastically by an amount $\epsilon_f L_0$. (c) Cracks formed in the film after exceeding elastic limit. (d) Cracks continue opening with increasing strain.

Figure 4: Variations of the average crack-spacing normalized to the film thickness versus strain-rate at four different temperatures. Two regimes of behavior are distinguishable.

Figure 5: Micrographs of cracked silica films on copper substrates strained at 500°C and various strain-rates: (a) $\dot{\epsilon} = 1.6 \times 10^{-3}$/s, (b) $\dot{\epsilon} = 8.3 \times 10^{-5}$/s, (c) $\dot{\epsilon} = 5 \times 10^{-5}$/s, (d) $\dot{\epsilon} = 2.7 \times 10^{-5}$/s. Films are shown in the steady-state regime. The parallel thick lines are the opening cracks. The dark lamellae are the silica strips still attached to the copper substrates. The increase of the crack-spacing with decreasing strain-rate can be noticed.

Figure 6: Variations of $\ln(\dot{\epsilon}\bar{\lambda})$ versus $\ln(t/\bar{\lambda})$ at two elevated temperatures. At 300°C, $n = 1.026$, at 500°C, $n = 0.961$.

Figure 7: Variations of $\dot{\epsilon}\bar{\lambda}^2/t$ versus strain-rate at two elevated temperatures, 300°C and 500°C.

Figure 8: The microscopic geometry of the copper-silica boundary is represented by a sine-wave of height h.

Figure 9: Variations of $\ln(\dot{\epsilon}\bar{\lambda}^2/t)$ versus $1/T$. Curve-fit of the type $\ln(\dot{\epsilon}\bar{\lambda}^2/t) = -a(1/T) + \ln(1/T) + b$.

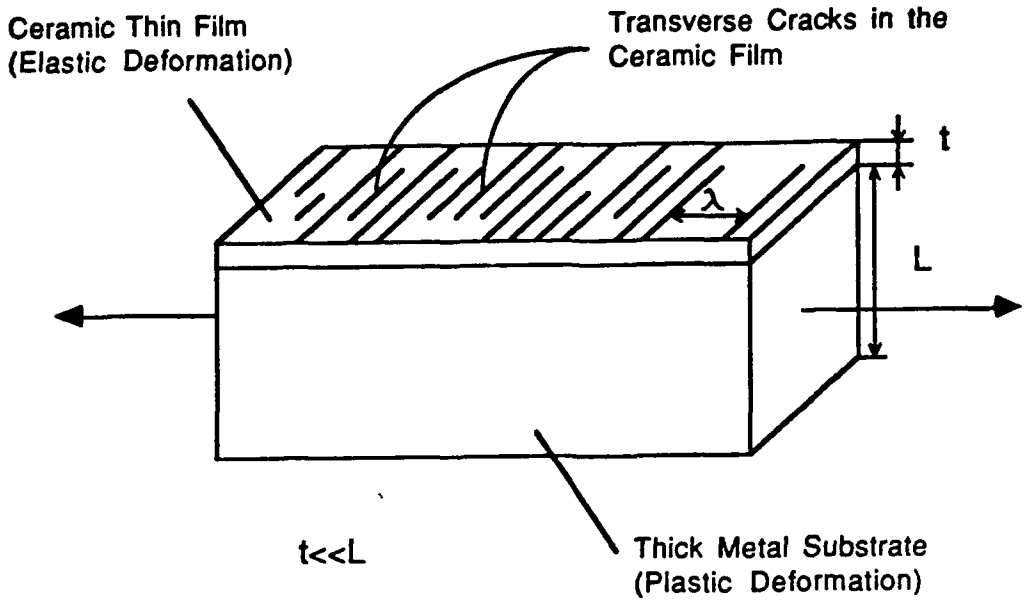
Ceramic Thin Film
(Elastic Deformation)
Transverse Cracks in the
Ceramic Film
t
λ
L
t<<L
Thick Metal Substrate
(Plastic Deformation)

(a)

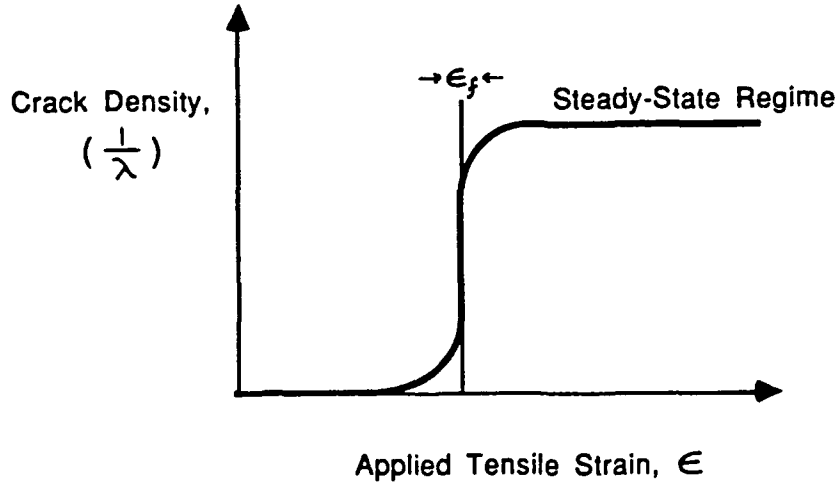
Crack Density,
(1/λ)
→ϵf←
Steady-State Regime
Applied Tensile Strain, ϵ

(b)

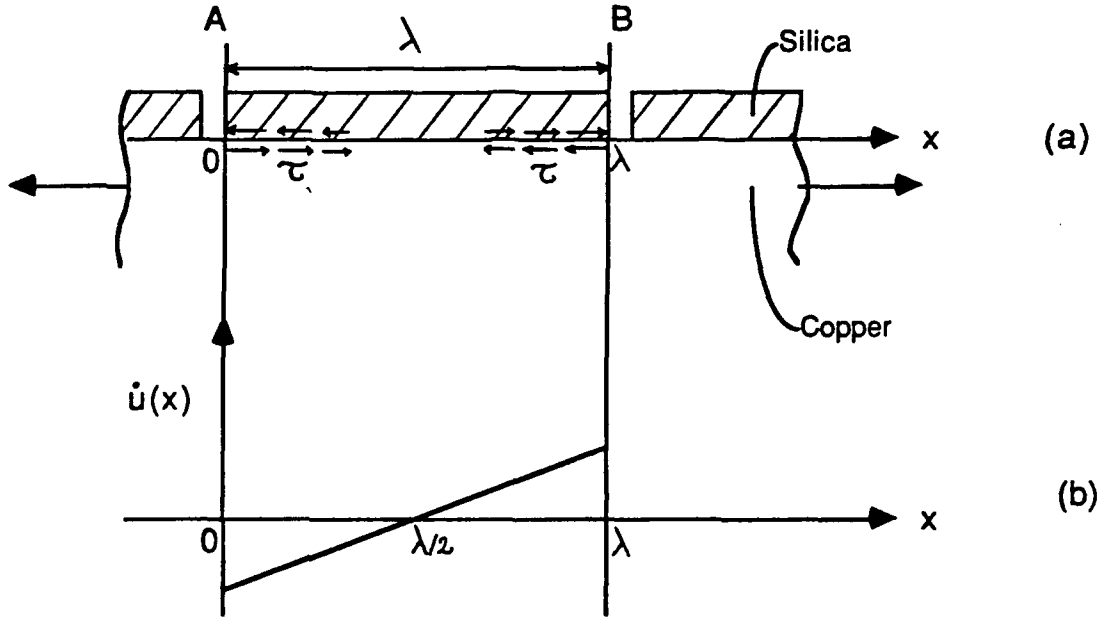
A
λ
B
Silica
x
(a)
0
τ
τ
λ
Copper
u̇(x)
(b)
x
0
λ/2
λ

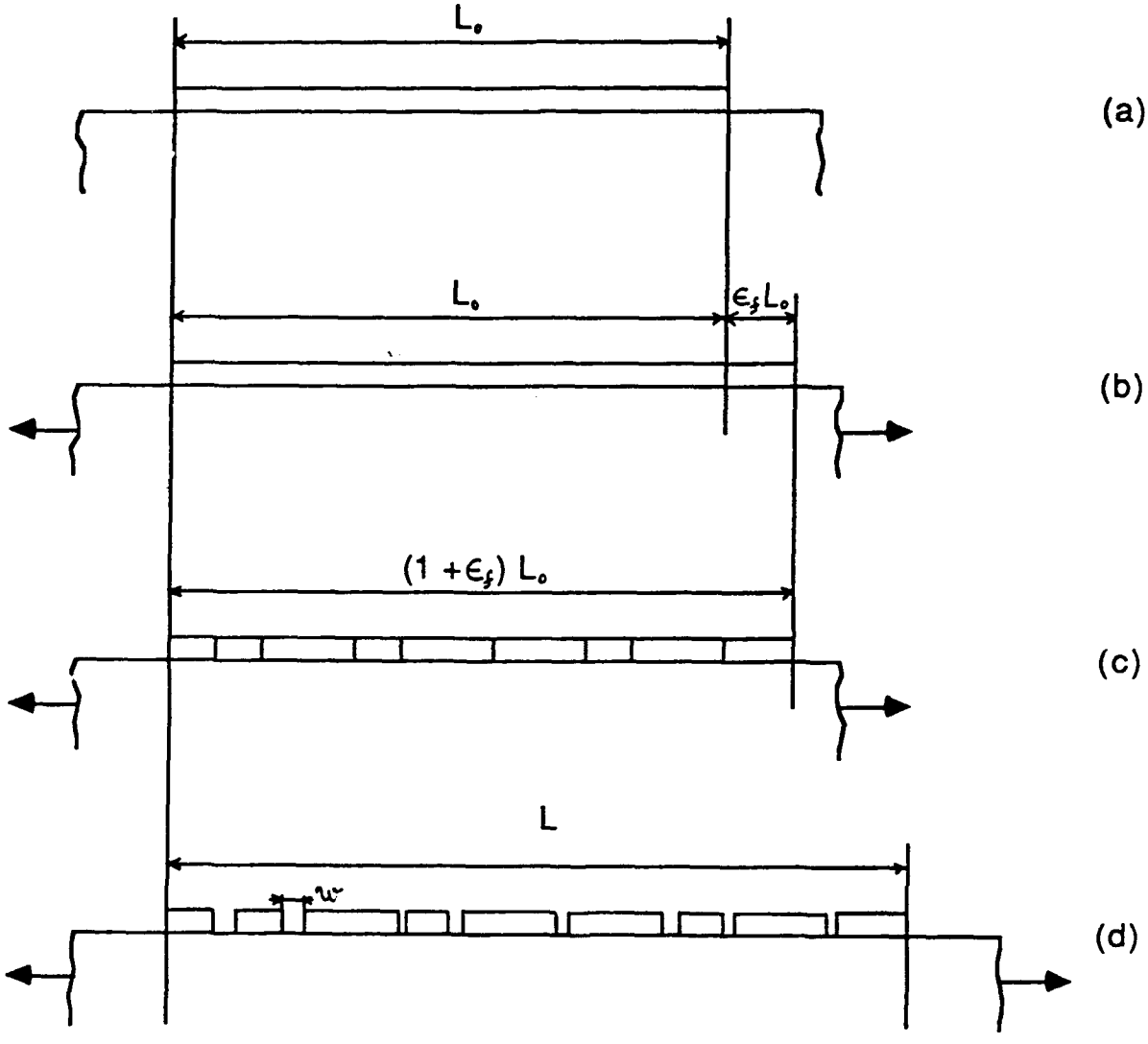
L_o
(a)
L_o
$\epsilon_f L_o$
(b)
$(1+\epsilon_f)\, L_o$
(c)
L
w
(d)

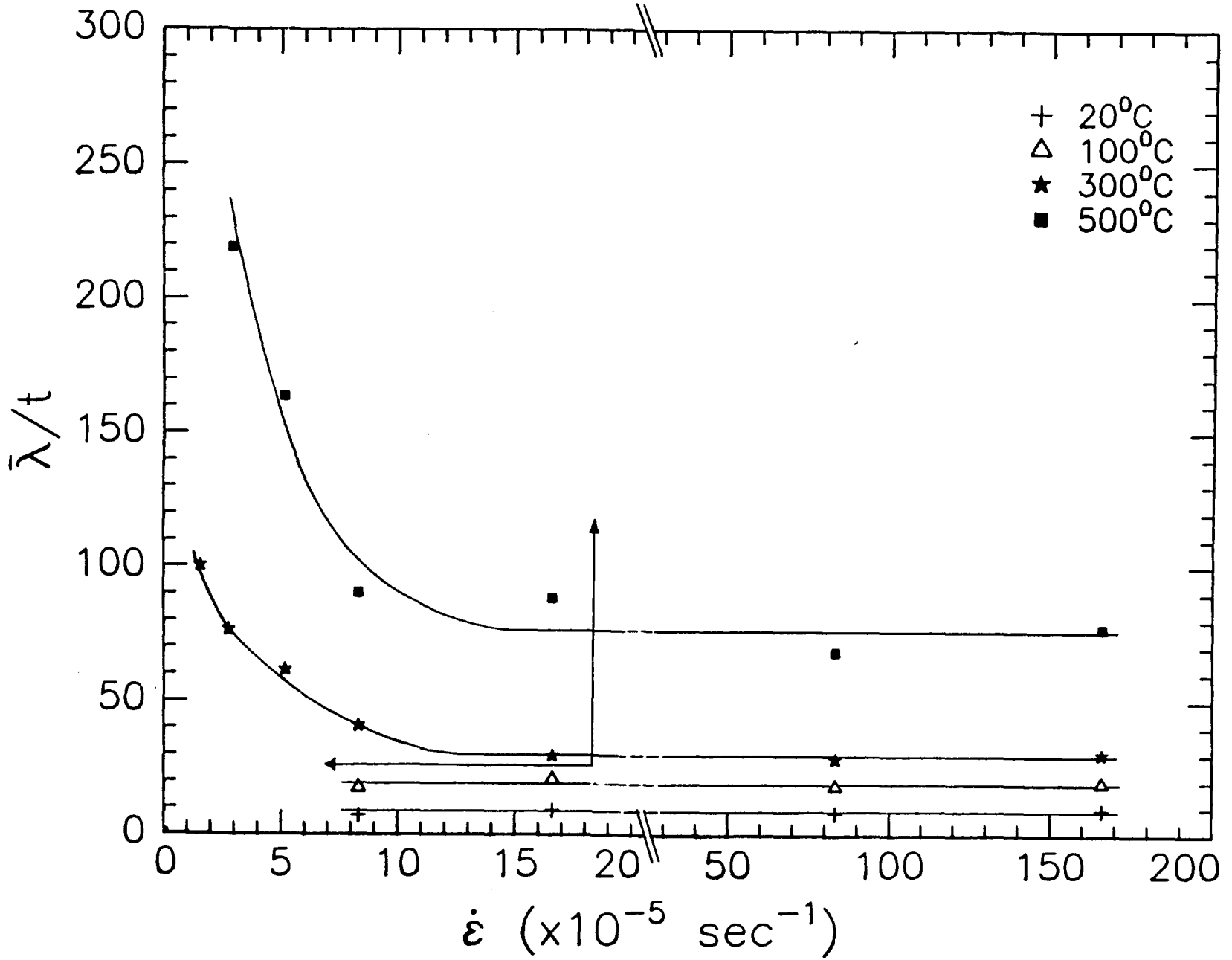
300
250
200
150
100
50
0
$\bar{\lambda}/t$
0
5
10
15
20
50
100
150
200
$\dot{\varepsilon}$ (x10^{-5} sec^{-1})
20°C
100°C
300°C
500°C

(a)

(b)

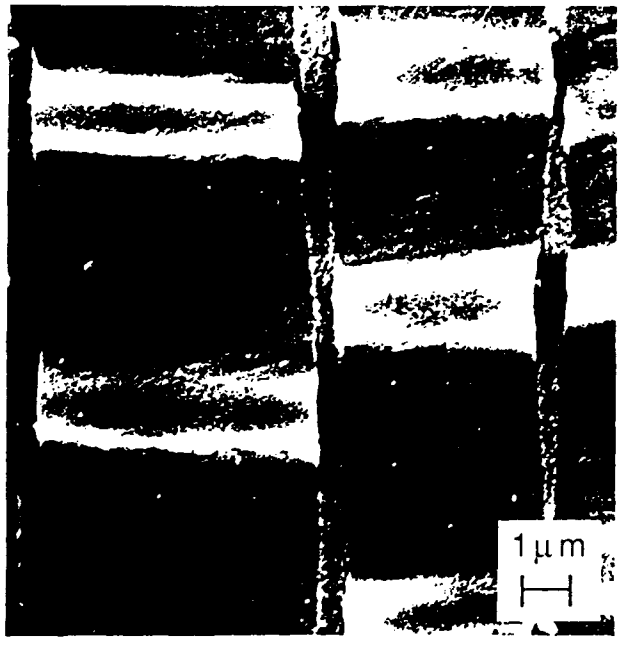

(c)

(d)

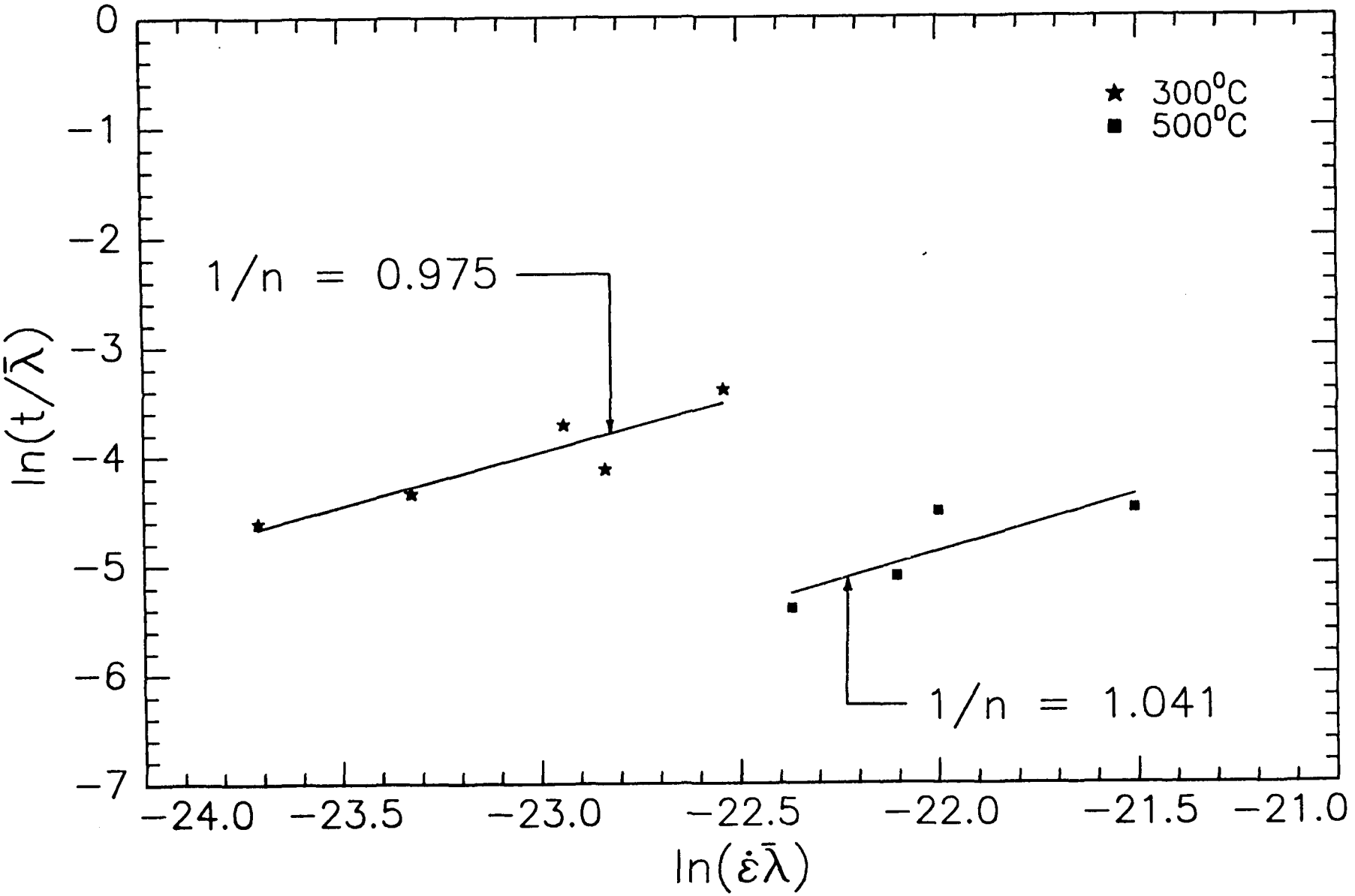
0
−1
−2
−3
−4
−5
−6
−7
−24.0
−23.5
−23.0
−22.5
−22.0
−21.5
−21.0
ln(t/λ̄)
ln(ε̇λ̄)
★ 300°C
■ 500°C
1/n = 0.975
1/n = 1.041

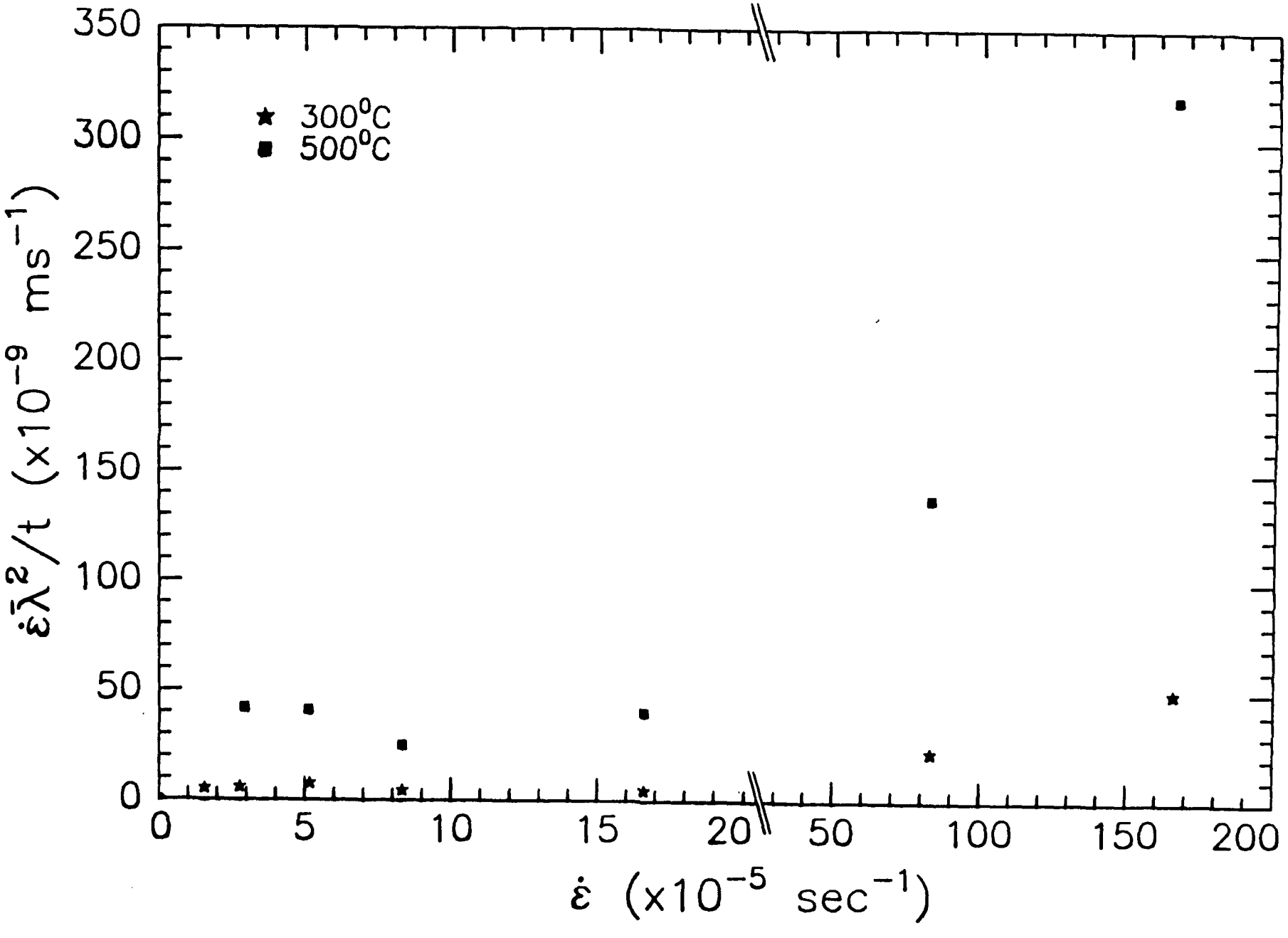
350
300
250
200
150
100
50
0
★ 300°C
■ 500°C
$\dot{\varepsilon}\bar{\lambda}^2/t$ (x10^{-9} ms^{-1})
0
5
10
15
20
50
100
150
200
$\dot{\varepsilon}$ (x10^{-5} sec^{-1})

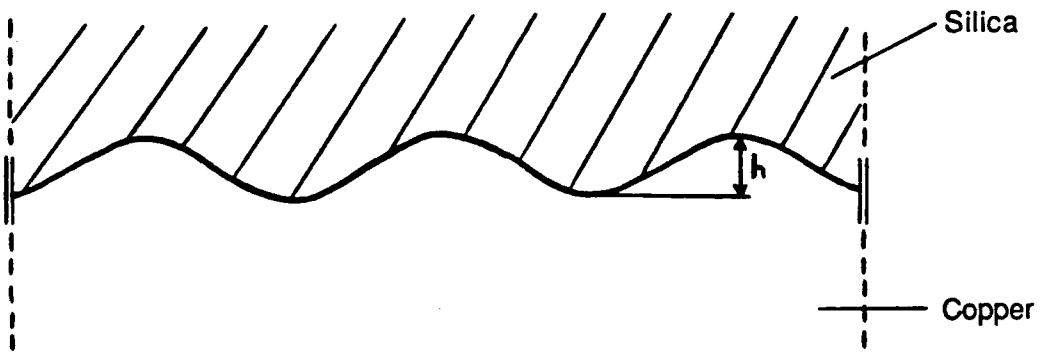
Silica
h
Copper

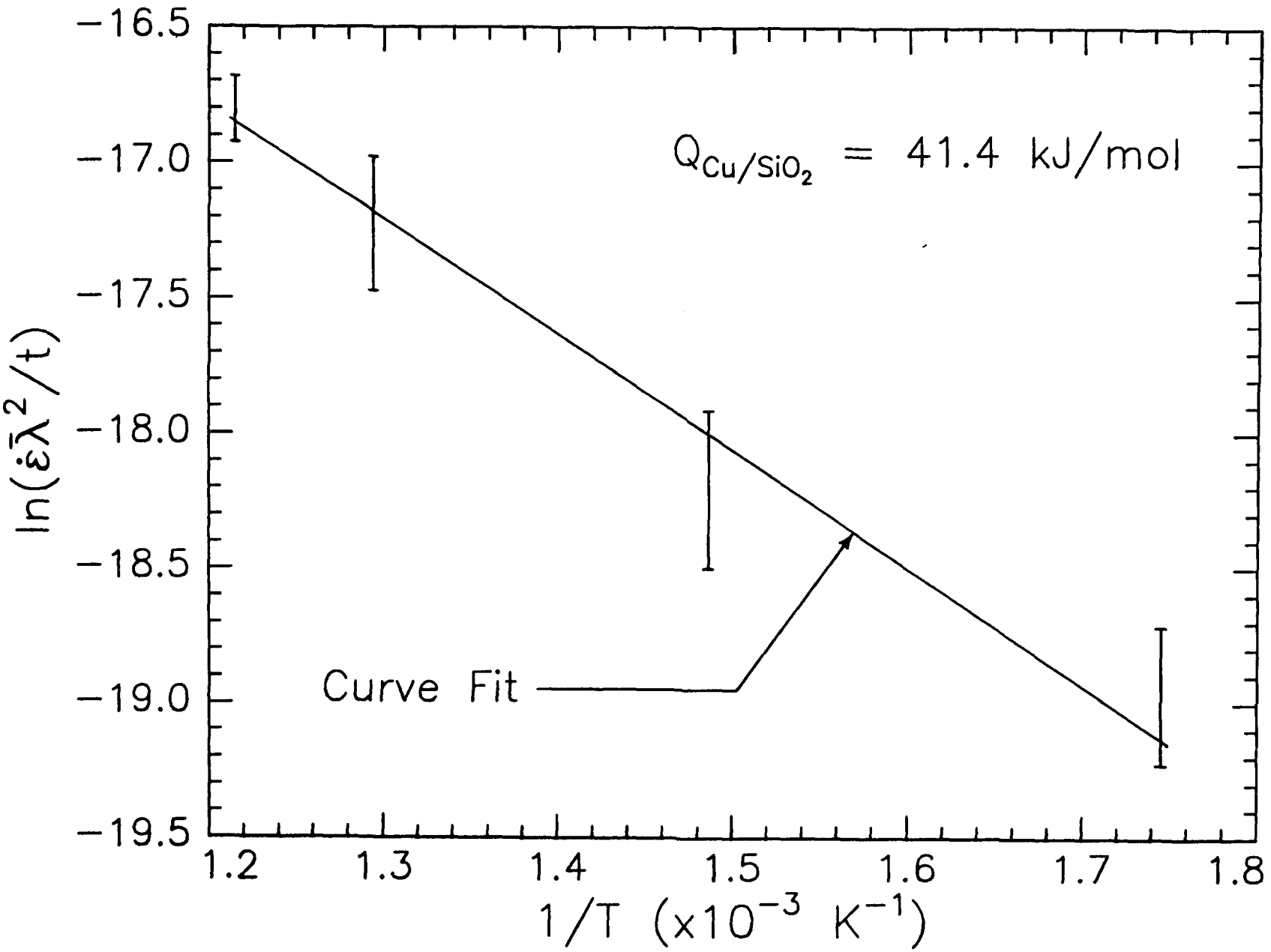
−16.5
−17.0
−17.5
−18.0
−18.5
−19.0
−19.5
$\ln(\dot{\varepsilon}\bar{\lambda}^2/t)$
Q_{Cu/SiO_2} = 41.4 kJ/mol
Curve Fit
1.2
1.3
1.4
1.5
1.6
1.7
1.8
1/T (x10^{-3} K^{-1})